CHAPTER 35
HELICAL GEARS

Raymond J. Drago, P.E.
Senior Engineer, Advanced Power Train Technology
Boeing Vertol Company
Philadelphia, Pennsylvania

The following is quoted from the Foreword of Ref. [35.1]:

> This AGMA Standard and related publications are based on typical or average data, conditions, or applications. The standards are subject to continual improvement, revision, or withdrawal as dictated by increased experience. Any person who refers to AGMA technical publications should be sure that he has the latest information available from the Association on the subject matter.
>
> Tables or other self-supporting sections may be quoted or extracted in their entirety. Credit line should read: "Extracted from ANSI/AGMA #2001-B88 Fundamental Rating Factors and Calculation Methods for Involute Spur and Helical Gear Teeth, with the permission of the publisher, American Gear Manufacturers Association, 1500 King Street, Alexandria, Virginia 22314."

This reference is cited because numerous American Gear Manufacturer's Association (AGMA) tables and figures are used in this chapter. In each case, the appropriate publication is noted in a footnote or figure caption.

35.1 INTRODUCTION

Helical gearing, in which the teeth are cut at an angle with respect to the axis of rotation, is a later development than spur gearing and has the advantage that the action is smoother and tends to be quieter. In addition, the load transmitted may be somewhat larger, or the life of the gears may be greater for the same loading, than with an equivalent pair of spur gears. Helical gears produce an end thrust along the axis of the shafts in addition to the separating and tangential (driving) loads of spur gears. Where suitable means can be provided to take this thrust, such as thrust collars or ball or tapered-roller bearings, it is no great disadvantage.

Conceptually, helical gears may be thought of as stepped spur gears in which the size of the step becomes infinitely small. For external parallel-axis helical gears to

mesh, they must have the same helix angle but be of different hand. An external-internal set will, however, have equal helix angle with the same hand.

Involute profiles are usually employed for helical gears, and the same comments made earlier about spur gears hold true for helical gears.

Although helical gears are most often used in a parallel-axis arrangement, they can also be mounted on nonparallel noncoplanar axes. Under such mounting conditions, they will, however, have limited load capacity.

Although helical gears which are used on crossed axes are identical in geometry and manufacture to those used on parallel axes, their operational characteristics are quite different. For this reason they are discussed separately at the end of this chapter. All the forthcoming discussion therefore applies only to helical gears operating on parallel axes.

35.2 TYPES

Helical gears may take several forms, as shown in Fig. 35.1:

1. Single
2. Double conventional
3. Double staggered
4. Continuous (herringbone)

Single-helix gears are readily manufactured on conventional gear cutting and grinding equipment. If the space between the two rows of a double-helix gear is wide enough, such a gear may also be cut and ground, if necessary, on conventional equipment. Continuous or herringbone gears, however, can be cut only on a special shaping machine (Sykes) and usually cannot be ground at all.

Only single-helix gears may be used in a crossed-axis configuration.

35.3 ADVANTAGES

There are three main reasons why helical rather than straight spur gears are used in a typical application. These are concerned with the noise level, the load capacity, and the manufacturing.

35.3.1 Noise

Helical gears produce less noise than spur gears of equivalent quality because the total contact ratio is increased. Figure 35.2 shows this effect quite dramatically. However, these results are measured at the mesh for a specific test setup; thus, although the trend is accurate, the absolute results are not.

Figure 35.2 also brings out another interesting point. At high values of helix angle, the improvement in noise tends to peak; that is, the curve flattens out. Had data been obtained at still higher levels, the curve would probably drop drastically. This is due to the difficulty in manufacturing and mounting such gears accurately enough to take full advantage of the improvement in contact ratio. These effects at

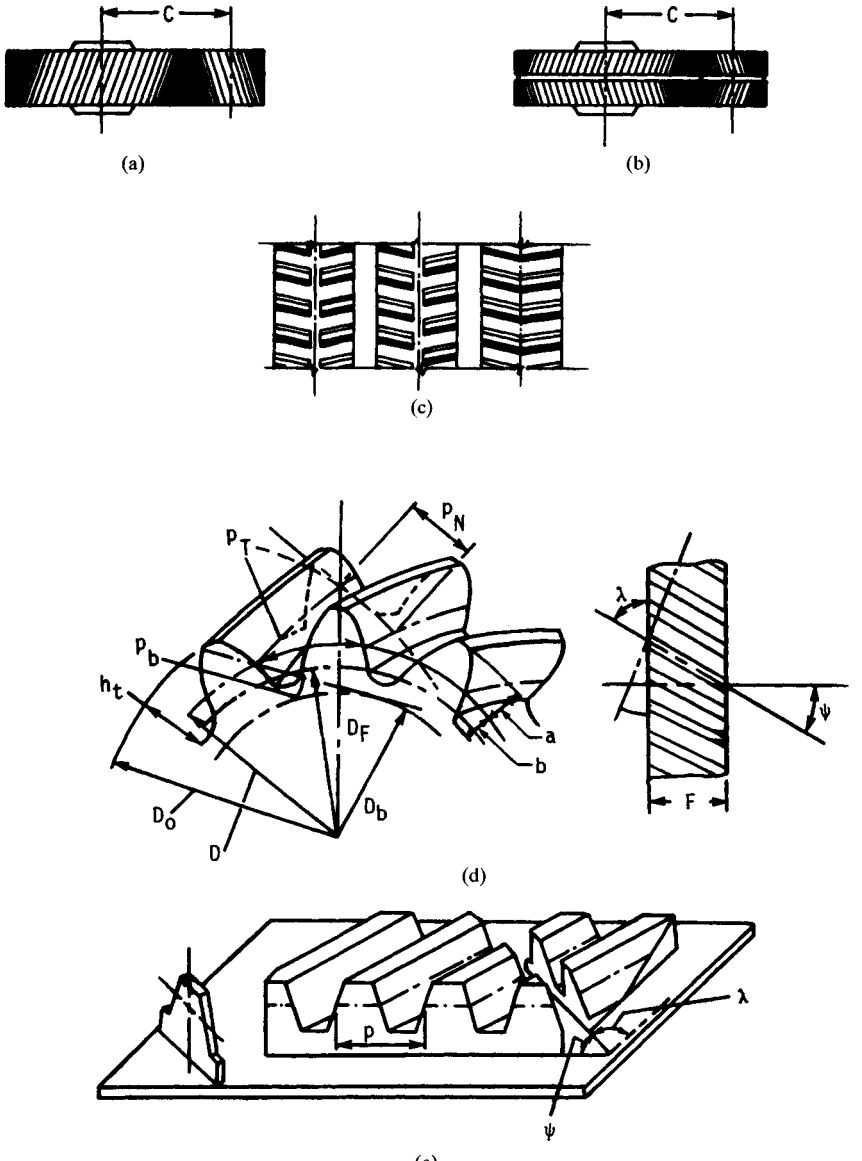

FIGURE 35.1 Terminology of helical gearing. (*a*) Single-helix gear. (*b*) Double-helix gear. (*c*) Types of double-helix gears: left, conventional; center, staggered; right, continous or herringbone. (*d*) Geometry. (*e*) Helical rack.

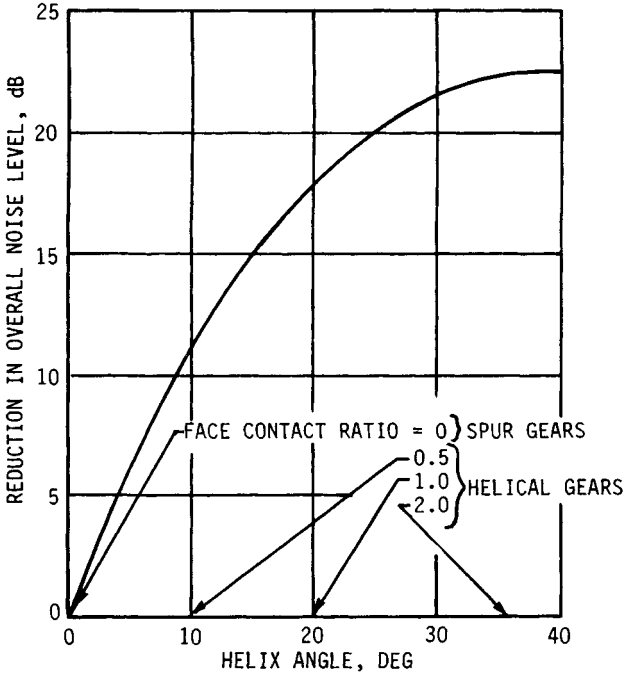

FIGURE 35.2 Effect of face-contact ratio on noise level. Note that increased helix angles lower the noise level.

very high helix angles actually tend to reduce the effective contact ratio, and so noise increases. Since helix angles greater than 45° are seldom used and are generally impractical to manufacture, this phenomenon is of academic interest only.

35.3.2 Load Capacity

As a result of the increased total area of tooth contact available, the load capacity of helical gears is generally higher than that of equivalent spur gears. The reason for this increase is obvious when we consider the contact line comparison which Fig. 35.3 shows. The most critical load condition for a spur gear occurs when a single tooth carries all the load at the highest point of single-tooth contact (Fig. 35.3*c*). In this case, the total length of the contact line is equal to the face width. In a helical gear, since the contact lines are inclined to the tooth with respect to the face width, the total length of the line of contact is increased (Fig. 35.3*b*), so that it is greater than the face width. This lowers unit loading and thus increases capacity.

35.3.3 Manufacturing

In the design of a gear system, it is often necessary to use a specific ratio on a specific center distance. Frequently this results in a diametral pitch which is nonstandard. If

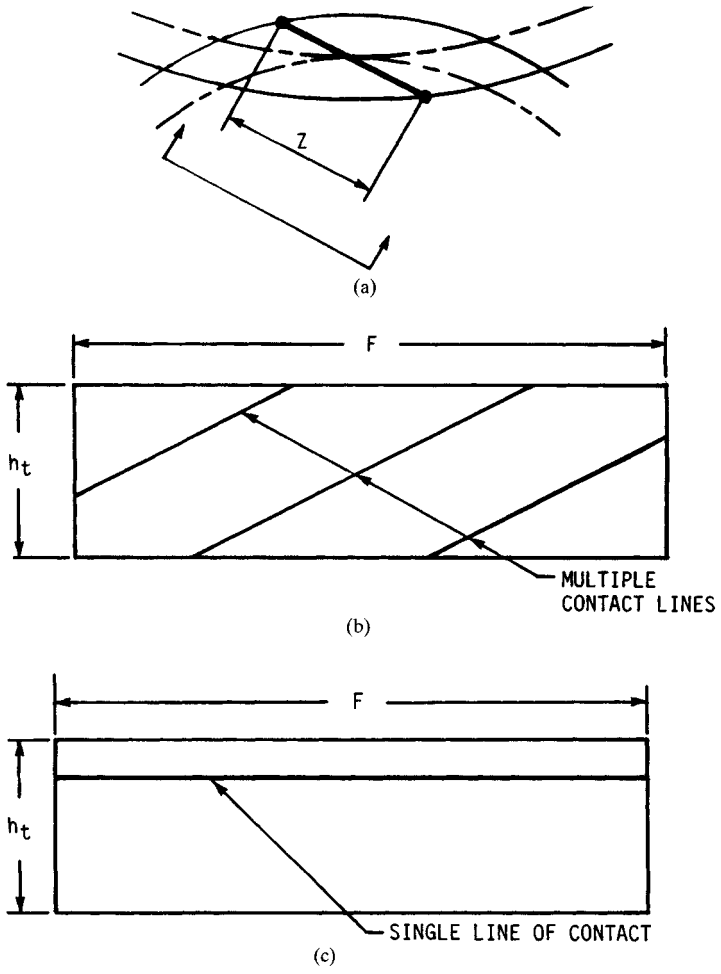

FIGURE 35.3 Comparison of spur and helical contact lines. (*a*) Transverse section; (*b*) helical contact lines; (*c*) spur contact line.

helical gears are employed, a limited number of standard cutters may be used to cut a wide variety of transverse-pitch gears simply by varying the helix angle, thus allowing virtually any center-distance and tooth-number combination to be accommodated.

35.4 GEOMETRY

When considered in the transverse plane (that is, a plane perpendicular to the axis of the gear), all helical-gear geometry is identical to that for spur gears. Standard tooth proportions are usually based on the normal diametral pitch, as shown in Table 35.1.

TABLE 35.1 Standard Tooth Proportions for Helical Gears

Quantity†	Formula	Quantity†	Formula
Addendum	$\frac{1.00}{P_N}$	External gears:	
Dedendum	$\frac{1.25}{P_N}$	Standard center distance	$\frac{D+d}{2}$
Pinion pitch diameter	$\frac{N_P}{P_N \cos \psi}$	Gear outside diameter	$D + 2a$
Gear pitch diameter	$\frac{N_G}{P_N \cos \psi}$	Pinion outside diameter	$d + 2a$
Normal arc tooth thickness	$\frac{\pi}{P_N} - \frac{B_N}{2}$	Gear root diameter	$D - 2b$
Pinion base diameter	$d \cos \phi_T$	Pinion root diameter	$d - 2b$
Gear base diameter	$D \cos \phi_T$	Internal gears: Center distance	$\frac{D-d}{2}$
Base helix angle	$\tan^{-1}(\tan \psi \cos \phi_T)$	Inside diameter	$d - 2a$
		Root diameter	$D + 2b$

†All dimensions in inches, and angles are in degrees.

It is frequently necessary to convert from the normal plane to the transverse plane and vice versa. Table 35.2 gives the necessary equations. All calculations previously defined for spur gears with respect to transverse or profile-contact ratio, top land, lowest point of contact, true involute form radius, nonstandard center, etc., are valid for helical gears if only a transverse plane section is considered.

For spur gears, the profile-contact ratio (ratio of contact to the base pitch) must be greater than unity for uniform rotary-motion transmission to occur. Helical gears, however, provide an additional overlap along the axial direction; thus their profile-contact ratio need not necessarily be greater than unity. The sum of both the profile-

TABLE 35.2 Conversions between Normal and Transverse Planes

Parameter (normal/transverse)	Normal to transverse	Transverse to normal
Pressure angle (ϕ_N/ϕ_T)	$\phi_T = \tan^{-1}\frac{\tan \phi_N}{\cos \psi}$	$\phi_N = \tan^{-1}(\tan \phi_T \cos \psi)$
Diametral pitch (P_N/P_d)	$P_d = P_N \cos \psi$	$P_N = \frac{P_d}{\cos \psi}$
Circular pitch (p_N/p_T)	$P_T = \frac{P_N}{\cos \psi}$	$P_N = P_T \cos \psi$
Arc tooth thickness (T_N/T_T)	$T_T = \frac{T_N}{\cos \psi}$	$T_N = T_T \cos \psi$
Backlash (B_N/B_T)	$B_T = \frac{B_N}{\cos \psi}$	$B_N = B_T \cos \psi$

contact ratio and the axial overlap must, however, be at least unity. The axial overlap, also often called the *face-contact ratio,* is the ratio of the face width to the axial pitch. The face-contact ratio is given by

$$m_F = \frac{P_{do} F \tan \psi_o}{\pi} \tag{35.1}$$

where P_{do} = operating transverse diametral pitch
ψ_o = helix angle at operating pitch circle
F = face width

Other parameters of interest in the design and analysis of helical gears are the base pitch p_b and the length of the line of action Z, both in the transverse plane. These are

$$p_b = \frac{\pi}{P_d} \cos \phi_T \tag{35.2}$$

and

$$Z = (r_o^2 - r_b^2)^{1/2} + (R_o^2 - R_b^2)^{1/2} - C_o \sin \phi_o \tag{35.3}$$

This equation is for an external gear mesh. For an internal gear mesh, the length of the line of action is

$$Z = (R_i^2 - R_b^2)^{1/2} - (r_o^2 - r_b^2)^{1/2} + C_o \sin \phi_o \tag{35.4}$$

where P_d = transverse diametral pitch as manufactured
ϕ_T = transverse pressure angle as manufactured, degrees (deg)
r_o = effective pinion outside radius, inches (in)
R_o = effective gear outside radius, in
R_i = effective gear inside radius, in
ϕ_o = operating transverse pressure angle, deg
r_b = pinion base radius, in
R_b = gear base radius, in
C_o = operating center distance, in

The operating transverse pressure angle ϕ_o is

$$\phi_o = \cos^{-1}\left(\frac{C}{C_o} \cos \phi_T\right) \tag{35.5}$$

The manufactured center distance C is simply

$$C = \frac{N_P + N_G}{2P_d} \tag{35.6}$$

for external mesh; for internal mesh, the relation is

$$C = \frac{N_G - N_P}{2P_d} \tag{35.7}$$

The contact ratio m_P in the transverse plane (profile-contact ratio) is defined as the ratio of the total length of the line of action in the transverse plane Z to the base pitch in the transverse plane p_b. Thus

$$m_P = \frac{Z}{p_b} \tag{35.8}$$

The diametral pitch, pitch diameters, helix angle, and normal pressure angle at the operating pitch circle are required in the load-capacity evaluation of helical gears. These terms are given by

$$P_{do} = \frac{N_P + N_G}{2C_o} \tag{35.9}$$

for external mesh; for internal mesh,

$$P_{do} = \frac{N_G - N_P}{2C_o} \tag{35.10}$$

Also,

$$d = \frac{N_P}{P_{do}} \qquad D = \frac{N_G}{P_{do}} \tag{35.11}$$

$$\psi_B = \tan^{-1}(\tan\psi \cos\phi_T) \tag{35.12}$$

$$\psi_o = \tan^{-1}\frac{\tan\psi_B}{\cos\phi_o} \tag{35.13}$$

$$\phi_{No} = \sin^{-1}(\sin\phi_o \cos\psi_B) \tag{35.14}$$

where P_{do} = operating diametral pitch
ψ_B = base helix angle, deg
ψ_o = helix angle at operating pitch point, deg
ϕ_{No} = operating normal pressure angle, deg
d = operating pinion pitch diameter, in
D = operating gear pitch diameter, in

35.5 LOAD RATING

Reference [35.1] establishes a coherent method for rating external helical and spur gears. The treatment of strength and durability provided here is derived in large part from this source.

Four factors must be considered in the load rating of a helical-gear set: strength, durability, wear resistance, and scoring probability. Although strength and durability must always be considered, wear resistance and scoring evaluations may not be required for every case. We treat each topic in some depth.

35.5.1 Strength and Durability

The strength of a gear tooth is evaluated by calculating the bending stress index number at the root by

$$s_t = \frac{W_t K_a}{K_v} \frac{P_d}{F_E} \frac{K_b K_m}{J} \tag{35.15}$$

where s_t = bending stress index number, pounds per square inch (psi)
K_a = bending application factor
F_E = effective face width, in
K_m = bending load-distribution factor
K_v = bending dynamic factor
J = bending geometry factor
P_d = transverse operating diametral pitch
K_b = rim thickness factor

The calculated bending stress index number s_t must be within safe operating limits as defined by

$$s_t \leq \frac{s_{at} K_L}{K_T K_R} \tag{35.16}$$

where s_{at} = allowable bending stress index number
K_L = life factor
K_T = temperature factor
K_R = reliability factor

Some of the factors which are used in these equations are similar to those used in the durability equations. Thus we present the basic durability rating equations before discussing the factors:

$$s_c = C_p \sqrt{\frac{W_t C_a}{C_v} \frac{1}{dF_N} \frac{C_m}{I}} \tag{35.17}$$

where s_c = contact stress index number
C_a = durability application factor
C_v = durability dynamic factor
d = operating pinion pitch diameter
F_N = net face width, in
C_m = load-distribution factor
C_p = elastic coefficient
I = durability geometry factor

The calculated contact stress index number must be within safe operating limits as defined by

$$s_c \leq \frac{s_{ac} C_L C_H}{C_T C_R} \tag{35.18}$$

where s_{ac} = allowable contact stress index number
C_L = durability life factor
C_H = hardness ratio factor
C_T = temperature factor
C_R = reliability factor

To utilize these equations, each factor must be evaluated. The tangential load W_t is given by

$$W_t = \frac{2T_P}{d} \tag{35.19}$$

where T_P = pinion torque in inch-pounds (in · lb) and d = pinion operating pitch diameter in inches. If the duty cycle is not uniform but does not vary substantially, then the maximum anticipated load should be used. Similarly, if the gear set is to operate at a combination of very high and very low loads, it should be evaluated at the maximum load. If, however, the loading varies over a well-defined range, then the cumulative fatigue damage for the loading cycle should be evaluated by using Miner's rule. For a good explanation, see Ref. [35.2].

Application Factors $\mathbf{C_a}$ ***and*** $\mathbf{K_a}$. The application factor makes the allowances for externally applied loads of unknown nature which are in excess of the nominal tangential load. Such factors can be defined only after considerable field experience has been established. In a *new* design, this consideration places the designer squarely on the horns of a dilemma, since "new" presupposes limited, if any, experience. The values shown in Table 35.3 may be used as a guide if no other basis is available.

TABLE 35.3 Application Factor Guidelines

	Character of load on driven machine		
Power source	Uniform	Moderate shock	Heavy shock
Uniform	1.15	1.25	At least 1.75
Light shock	1.25	1.50	At least 2.00
Medium shock	1.50	1.75	At least 2.50

The application factor should never be set equal to unity except where clear experimental evidence indicates that the loading will be absolutely uniform. Wherever possible, the actual loading to be applied to the system should be defined. One of the most common mistakes made by gear system designers is assuming that the motor (or engine, etc.) "nameplate" rating is also the gear unit rating point.

Dynamic Factors $\mathbf{C_v}$ ***and*** $\mathbf{K_v}$. These factors account for internally generated tooth loads which are induced by nonconjugate meshing action. This discontinuous motion occurs as a result of various tooth errors (such as spacing, profile, and runout) and system effects (such as deflections). Other effects, such as system torsional resonances and gear blank resonant responses, may also contribute to the overall dynamic loading experienced by the teeth. The latter effects must, however, be separately evaluated. The effect of tooth accuracy may be determined from Fig. 35.4, which is based on both pitch line velocity and gear quality Q_n as specified in Ref. [35.3]. The pitch line velocity of a gear is

$$v_t = 0.2618nD \tag{35.20}$$

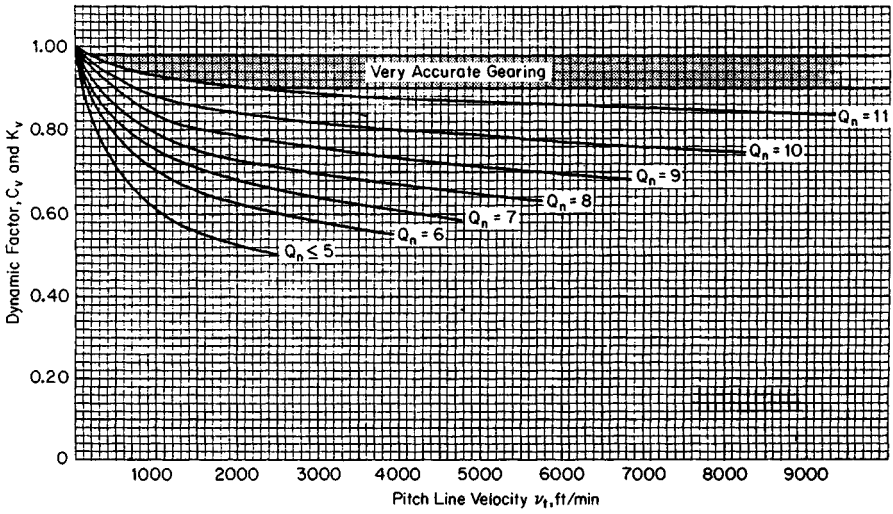

FIGURE 35.4 Dynamic factors C_v and K_v. *(From Ref. [35.1].)*

where v_t = pitch line velocity, feet per minute (ft/min)
n = gear speed, revolutions per minute (r/min)
D = gear pitch diameter, in

Effective and Net Face Widths $\mathbf{F_E}$ ***and*** $\mathbf{F_N}$. The net minimum face width of the narrowest member should always be used for F_N. In cases where one member has a substantially larger face width than its mate, some advantage may be taken of this fact in the bending stress calculations, but it is unlikely that a very narrow tooth will fully transfer its tooth load across the face width of a much wider gear. At best, the effective face width of a larger-face-width gear mating with a smaller-face-width gear is limited to the minimum face of the smaller member plus some allowance for the extra support provided by the wide face. Figure 35.5 illustrates the definition of net and effective face widths for various cases.

Rim Thickness Factor $\mathbf{K_b}$. The basic bending stress equations were developed for a single tooth mounted on a rigid support so that it behaves as a short cantilever beam. As the rim which supports the gear tooth becomes thinner, a point is reached at which the rim no longer provides "rigid" support. When this occurs, the bending of the rim itself combines with the tooth bending to yield higher total alternating stresses than would be predicted by the normal equations. Additionally, when a tooth is subjected to fully reversed bending loads, the alternating stress is also increased because of the additive effect of the compressive stress distribution on the normally unloaded side of the tooth, as Fig. 35.6 shows. Both effects are accounted for by the rim thickness factor, as Fig. 35.7 indicates.

It must be emphasized that the data shown in Fig. 35.7 are based on a limited amount of analytical and experimental (photoelastic and strain-gauge) measurements and thus must be used judiciously. Still, they are the best data available to date and are far better than nothing at all; see Refs. [35.4] and [35.5].

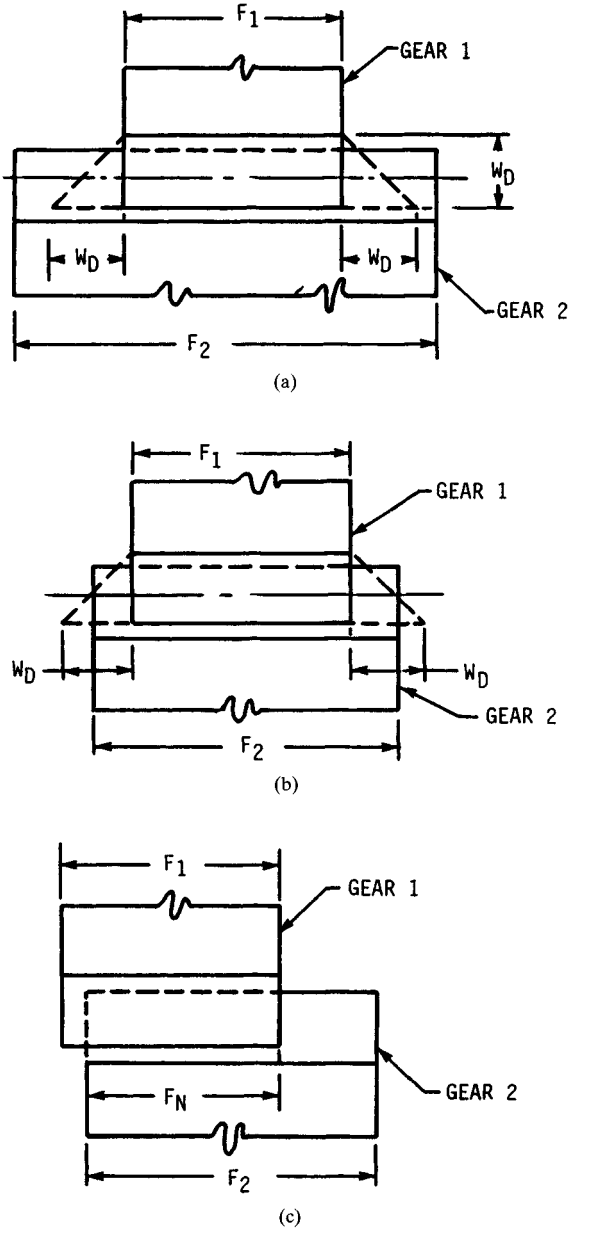

FIGURE 35.5 Definition of effective face width. (*a*) $F_{E1} = F_1, F_{E2} = F_1 + 2W_D$; $F_N = F_1$; (*b*) $F_{E1} = F_1, F_{E2} = F_2, F_N = F_1$; (*c*) $F_{E1} = F_{E2} = F_N$.

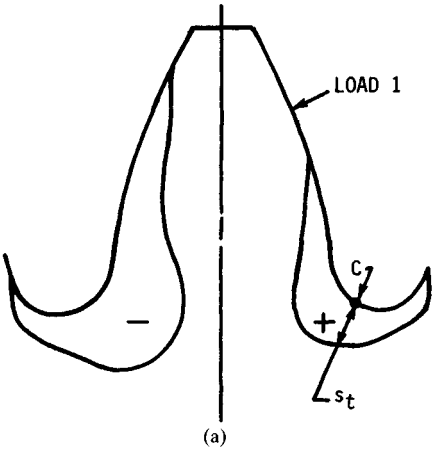

(a)

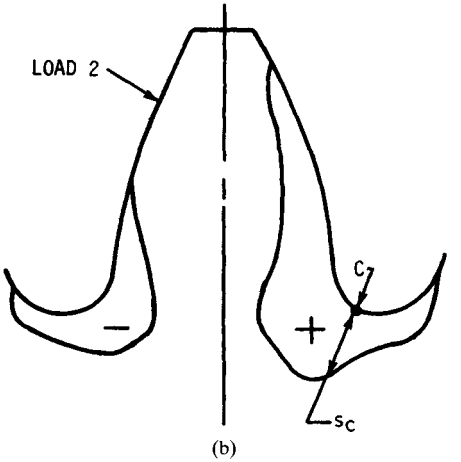

(b)

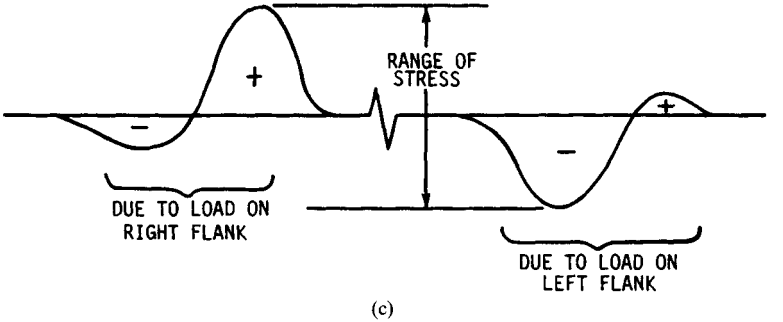

(c)

FIGURE 35.6 Stress condition for reversing (as with an idler) loading. (*a*) Load on right flank; (*b*) load on left flank; (*c*) typical waveform for strain gauge at point *C*.

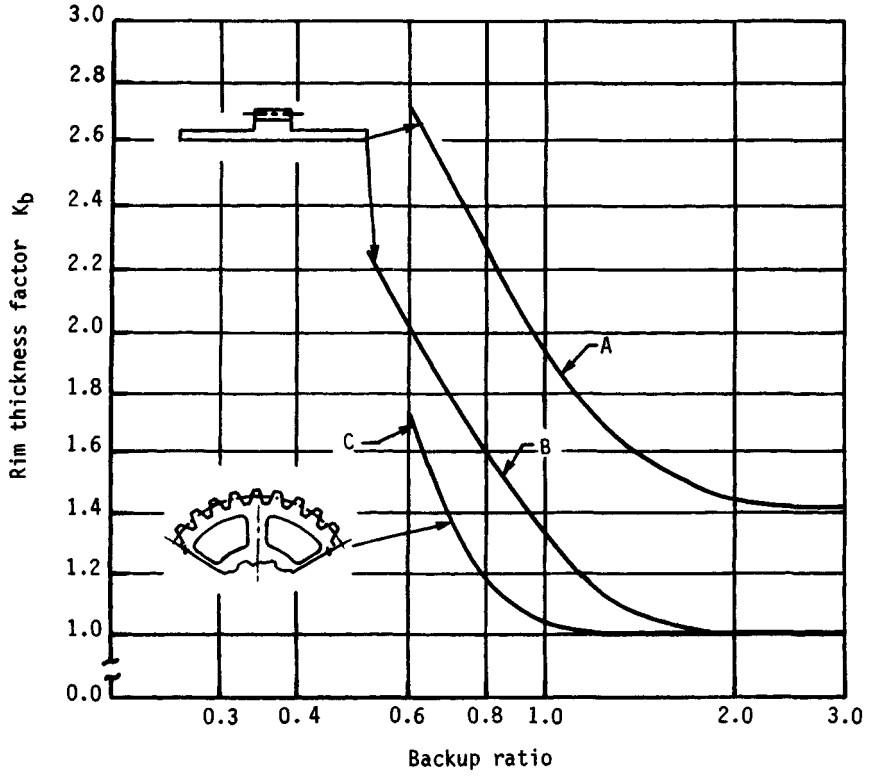

FIGURE 35.7 Rim thickness factor K_b. The *backup ratio* is defined as the ratio of the rim thickness to the tooth height. Curve *A* is fully reversed loading; curves *B* and *C* are unidirectional loading.

For gear blanks which utilize a T-shaped rim and web construction, the web acts as a hard point, if the rim is thin, and stresses will be higher over the web than over the ends of the T. The actual value which should be used for such constructions depends greatly on the relative proportions of the gear face width and the web. If the web spans 70 to 80 percent of the face width, the gear may be considered as having a rigid backup. Thus the backup ratio will be greater than 2.0, and any of the curves shown may be used (that is, curve *C* or *B*, both of which are identical above a 2.0 backup ratio, for unidirectional loading or curve *A* for fully reversed loading). If the proportions are between these limits, the gear lies in a gray area and probably lies somewhere in the range defined by curves *B* and *C*. Some designer discretion should be exercised here.

Finally, note that the rim thickness factor is equal to unity only for unidirectionally loaded, rigid-backup helical gears. For fully reversed loading, its value will be at least 1.4, even if the backup is rigid.

Load-Distribution Factors $\mathbf{K_m}$ ***and*** $\mathbf{C_c}$. These factors modify the rating equations to account for the manner in which the load is distributed on the teeth. The load on a set of gears will never be exactly uniformly distributed. Factors which affect the load distribution include the accuracy of the teeth themselves; the accuracy of the

housing which supports the teeth (as it influences the alignment of the gear axes); the deflections of the housing, shafts, and gear blanks (both elastic and thermal); and the internal clearances in the bearings which support the gears, among others.

All these and any other appropriate effects must be evaluated in order to define the total effective alignment error e_t for the gear pair. Once this is accomplished, the load-distribution factor may be calculated.

In some cases it may not be possible to fully define or even estimate the value of e_t. In such cases an empirical approach may be used. We discuss both approaches in some detail.

The empirical approach requires only minimal data, and so it is the simplest to apply. Several conditions must be met, however, prior to using this method:

1. Net face width to pinion pitch diameter ratios must be less than or equal to 2.0. (For double-helix gears, the gap is not included in the face width.)
2. The gear elements are mounted between bearings (not overhung).
3. Face width can be up to 40 in.
4. There must be contact across the full face width of the narrowest member when loaded.
5. Gears are not highly crowned.

The empirical expression for the load-distribution factor is

$$C_m = K_m = 1.0 + C_{mc}(C_{pf}C_{pm} + C_{ma}C_e) \tag{35.21}$$

where C_{mc} = lead correction factor
C_{pf} = pinion proportion factor
C_{pm} = pinion proportion modifier
C_{ma} = mesh alignment factor
C_e = mesh alignment correction factor

The lead correction factor C_{mc} modifies the peak loading in the presence of slight crowning or lead correction as follows:

$$C_{mc} = \begin{cases} 1.0 & \text{for gear with unmodified leads} \\ 0.8 & \text{for gear with leads properly modified by crowning or lead correction} \end{cases}$$

Figure 35.8 shows the pinion proportion factor C_{pf}, which accounts for deflections due to load. The pinion proportion modifier C_{pm} alters C_{pf} based on the location of the pinion relative to the supporting bearings. Figure 35.9 defines the factors S and S_1. And C_{pm} is defined as follows:

$$C_{pm} = \begin{cases} 1.0 & \text{when } S_1/S < 0.175 \\ 1.1 & \text{when } S_1/S \geq 0.175 \end{cases}$$

The mesh alignment factor C_{ma} accounts for factors other than elastic deformations. Figure 35.10 provides values for this factor for four accuracy groupings. For double-helix gears, this figure should be used with F equal to half of the total face width. The mesh alignment correction factor C_e modifies the mesh alignment factor to allow for the improved alignment which may be obtained when a gear set is adjusted at assembly or when the gears are modified by grinding, skiving, or lapping to more closely match their mates at assembly (in which case, pinion and gear

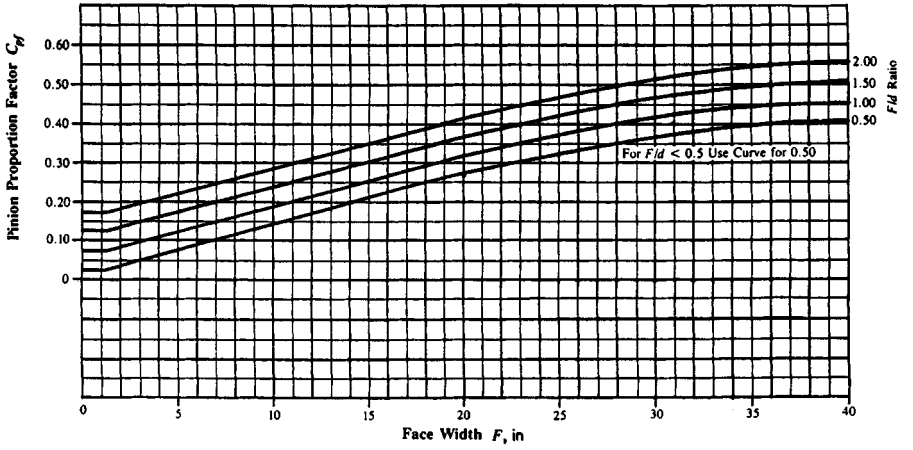

FIGURE 35.8 Pinion proportion factor C_{pf}. *(From Ref. [35.1].)*

become a matched set). Only two values are permissible for C_e—either 1.0 or 0.8, as defined by the following requirements:

$$C_e = \begin{cases} 0.80 & \text{when the compatibility of the gearing is improved by lapping, grinding, or skiving after trial assembly to improve contact} \\ 0.80 & \text{when gearing is adjusted at assembly by shimming support bearings and/or housing to yield uniform contact} \\ 1.0 & \text{for all other conditions} \end{cases}$$

If enough detailed information is available, a better estimate of the load-distribution factor may be obtained by using a more analytical approach. This method, however, requires that the total alignment error e_t be calculated or estimated. Depending on the contact conditions, one of two expressions is used to calculate the load-distribution factor.

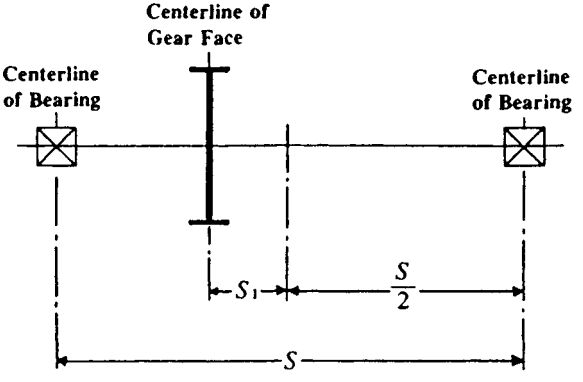

FIGURE 35.9 Definition of distances S and S_1. Bearing span is distance S; pinion offset from midspan is S_1. *(From Ref. [35.1].)*

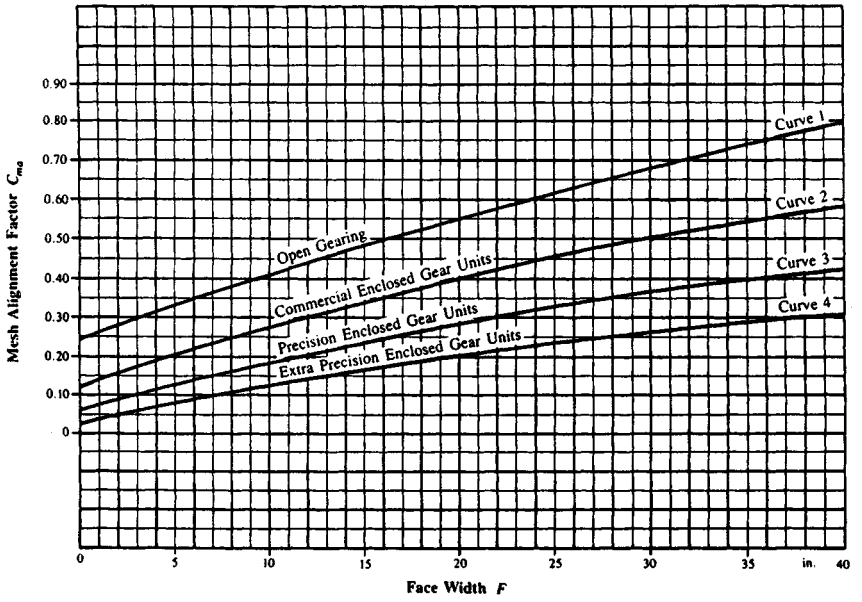

FIGURE 35.10 Mesh alignment factor C_{ma}. For analytical method for determination of C_{ma}, see Eq. (35.21). *(From Ref. [35.1].)*

If the tooth contact pattern at normal operating load essentially covers the entire available tooth face, Eq. (35.22) should be used. If the tooth contact pattern does not cover the entire available tooth face (as would be the case for poorly aligned or high-crowned gears) at normal operating loads, then Eq. (35.23) must be used:

$$C_m = 1.0 + \frac{Ge_tZF}{4W_t p_b} \tag{35.22}$$

and

$$C_m = \sqrt{\frac{Ge_tZF}{W_t p_b}} \tag{35.23}$$

where W_t = tangential tooth load, pounds (lb)
G = tooth stiffness constant, (lb/in)/in of face
Z = length of line of contact in transverse plane
e_t = total effective alignment error, in/in
p_b = transverse base pitch, in
F = net face width of narrowest member, in

The value of G will vary with tooth proportions, tooth thickness, and material. For steel gears of standard or close to standard proportions, it is normally in the range of 1.5×10^6 to 2.0×10^6 psi. The higher value should be used for higher-pressure-angle teeth, which are normally stiffer, while the lower value is representative of more flexible teeth. The most conservative approach is to use the higher value in all cases.

For double-helix gears, each half should be analyzed separately by using the appropriate values of F and e_t and by assuming that half of the tangential tooth load is transmitted by each half (the values for p_b, Z, and G remain unchanged).

***Geometry Factor* I.** The geometry factor I evaluates the radii of curvature of the contacting tooth profiles based on the pressure angle, helix, and gear ratio. Effects of modified tooth proportions and load sharing are considered. The I factor is defined as follows:

$$I = \frac{C_c C_x C_\psi^2}{m_N} \tag{35.24}$$

where C_c = curvature factor at operating pitch line
C_x = contact height factor
C_ψ = helical overlap factor
m_N = load-sharing ratio

The curvature factor is

$$C_c = \frac{\cos \phi_o \sin \phi_o}{2} \frac{N_G}{N_G + N_P} \tag{35.25}$$

for external mesh; for internal mesh,

$$C_c = \frac{\cos \phi_o \sin \phi_o}{2} \frac{N_G}{N_G - N_P} \tag{35.26}$$

The contact height factor C_x adjusts the location on the tooth profile at which the critical contact stress occurs (i.e., face-contact ratio > 1.0). The stress is calculated at the mean diameter or the middle of the tooth profile. For low-contact-ratio helical gears (that is, face-contact ratio ≤ 1.0), the stress is calculated at the lowest point of single-tooth contact in the transverse plane and C_x is given by Eq. (35.27):

$$C_x = \frac{R_1 R_2}{R_P R_G} \tag{35.27}$$

where R_P = pinion curvature radius at operating pitch point, in
R_G = gear curvature radius at operating pitch point, in
R_1 = pinion curvature radius at critical contact point, in
R_2 = gear curvature radius at critical contact point, in

The required radii are given by

$$R_P = \frac{d}{2} \sin \phi_o \qquad R_G = \frac{D}{2} \sin \phi_o \tag{35.28}$$

where d = pinion operating pitch diameter, in
D = gear operating pitch diameter, in
ϕ_o = operating pressure angle in transverse plane, deg

$$R_1 = R_P - Z_c \tag{35.29}$$

and

$$R_2 = R_G + Z_c \tag{35.30}$$

for external gears; for internal gears,

$$R_2 = R_G - Z_c \tag{35.31}$$

where Z_c is the distance along the line of action in the transverse plane to the critical contact point. The value of Z_c is dependent on the transverse contact ratio. For helical gears where the face-contact ratio ≤ 1.0, Z_c is found by using Eq. (35.32). For normal helical gears where the face-contact ratio is > 1.0, Eq. (35.33) is used:

$$Z_c = p_b - 0.5[(d_o^2 - d_b^2)^{1/2} - (d^2 - d_b^2)^{1/2}] \qquad m_F \le 1.0 \tag{35.32}$$

and

$$Z_c = 0.5\,[(d^2 - d_b^2)^{1/2} - (d_m^2 - d_b^2)^{1/2}] \qquad m_F > 1.0 \tag{35.33}$$

where p_b = base pitch, in
d_o = pinion outside diameter, in
d_b = pinion base diameter, in
d_m = pinion mean diameter, in

The pinion mean diameter is defined by Eq. (35.34) or (35.35). For external mesh,

$$d_m = C_o - \frac{D_o - d_o}{2} \tag{35.34}$$

For internal mesh,

$$d_m = \frac{D_I + d_o}{2} - C_o \tag{35.35}$$

where D_o = external gear outside diameter and D_I = internal gear inside diameter.

The helical factor C_ψ accounts for the partial helical overlap action which occurs in helical gears with a face-contact ratio $m_F \le 1.0$. For helical gears with a face-contact ratio > 1.0, C_ψ is set equal to unity; for low-contact helical gears, it is

$$C_\psi = \sqrt{1 - m_F + \frac{C_{xn} Z m_F^2}{C_x F \sin \psi_b}} \tag{35.36}$$

where Z = total length of line of action in transverse plane, in
F = net minimum face width, in
m_F = face-contact ratio
C_x = contact height factor [Eq. (35.27)]
C_{xn} = contact height factor for equivalent normal helical gears [Eq. (35.37)]
ψ_b = base helix angle, deg

The C_{xn} factor is given by

$$C_{xn} = \frac{R_{1n} R_{2n}}{R_P R_G} \tag{35.37}$$

where R_{1n} = curvature radius at critical point for equivalent normal helical pinion, in
R_{2n} = curvature radius at critical contact point for equivalent normal helical gear, in

The curvature radii are given by

$$R_{1n} = R_P - Z_c \tag{35.38}$$

$$\begin{aligned} R_{2n} &= R_G + Z \qquad \text{external gears} \\ R_{2n} &= R_G - Z_c \qquad \text{internal gears} \end{aligned} \tag{35.39}$$

where Eq. (35.38) applies to external gears and Eq. (35.39) to either, as appropriate. Also, the term Z_c is obtained from Eq. (35.32).

The load-sharing ratio m_N is the ratio of the face width to the minimum total length of the contact lines:

$$m_N = \frac{F}{L_{\min}} \tag{35.40}$$

where m_N = load-sharing ratio
F = minimum net face width, in
$L_{\min}$ = minimum total length of contact lines, in

The calculation of $L_{\min}$ is a rather involved process. For most helical gears which have a face-contact ratio of at least 2.0, a conservative approximation for the load-sharing ratio ratio m_N may be obtained from

$$m_N = \frac{P_N}{0.95Z} \tag{35.41}$$

where p_N = normal circular pitch in inches and Z = length of line of action in the transverse plane in inches. For helical gears with a face-contact ratio of less than 2.0, it is imperative that the actual value of $L_{\min}$ be calculated and used in Eq. (35.40). The method for doing this is shown in Eqs. (35.42) through (35.45):

$$L_{\min} = \frac{1}{\sin \psi_b} [(P_1 - Q_1) + (P_2 - Q_2) + \cdots + (P_i - Q_i) + \cdots + (P_n - Q_n)] \tag{35.42}$$

where n = limiting number of lines of contact, as given by

$$n = \frac{(Z/\tan \psi_b) + F}{p_x} \tag{35.43}$$

Also, P_i = sum of base pitches in inches. The ith term of P_i is the lesser of

$$ip_x \tan \psi_b \qquad \text{or} \qquad Z \tag{35.44}$$

Finally, Q_i = remainder of base pitches in inches. Its value is

$$Q_i = 0 \qquad \text{if } ip_x \le F$$

But when $ip_x > F$, then Q_i is the ith term and is the lesser of

$$(ip_x - F) \tan \psi_b \qquad \text{or} \qquad Z \tag{35.45}$$

***Geometry Factor* J.** The bending strength geometry factor is

$$J = \frac{YC_\psi}{K_f m_N} \tag{35.46}$$

where Y = tooth form factor
K_f = stress correction factor
C_ψ = helical factor
m_N = load-distribution factor

The helical and load-distribution factors were both defined in the discussion of the geometry factor *I*. The calculation of Y is also a long, tedious process. For helical gears in which load sharing exists among the teeth in contact and for which the face-contact ratio is at least 2.0, the value of Y need not be calculated, since the value for J may be obtained directly from the charts shown in Figs. 35.11 through 35.25 with Eq. (35.47):

$$J = J' Q_{TR} Q_{TT} Q_A Q_H \tag{35.47}$$

where J' = basic geometry factor
Q_{TR} = tool radius adjustment factor
Q_{TT} = tooth thickness adjustment factor
Q_A = addendum adjustment factor
Q_H = helix-angle adjustment factor

In using these charts, note that the values of addendum, dedendum, and tool-tip radius are given for a 1-normal-pitch gear. Values for any other pitch may be obtained by dividing the factor by the actual normal diametral pitch. For example, if an 8-normal-pitch gear is being considered, the parameters shown on Fig. 35.11 are

$$\text{Addendum } a = \frac{1.0}{8} = 0.125 \text{ in}$$

$$\text{Dedendum } b = \frac{1.35}{8} = 0.168\,75 \text{ in}$$

$$\text{Tool (hob) tip radius } r_T = \frac{0.42}{8} = 0.0525 \text{ in}$$

The basic geometry factor J' is found from Figs. 35.11 through 35.25. The tool radius adjustment factor Q_{TR} is found from Figs. 35.14 through 35.16 if the edge radius on the tool is other than $0.42/P_d$, which is the standard value used in calculating J'. Similarly, for gears with addenda other than $1.0/P_d$ or tooth thicknesses other than the standard value of $\pi/(2P_d)$, the appropriate factors may be obtained from these charts. In the case of a helical gear, the adjustment factor Q_H is obtained from Figs. 35.23 through 35.25. If a standard helical gear is being considered, Q_{TR}, Q_{TT}, and Q_A remain equal to unity, but Q_H must be found from Figs. 35.23 to 35.25.

These charts are computer-generated and, when properly used, produce quite accurate results. Note that they are also valid for spur gears if Q_H is set equal to unity (that is, enter Figs. 35.23 through 35.25 with 0° helix angle).

The charts shown in Figs. 35.11 through 35.25 assume the use of a standard full-radius hob. Additional charts, still under the assumption that the face-contact ratio is

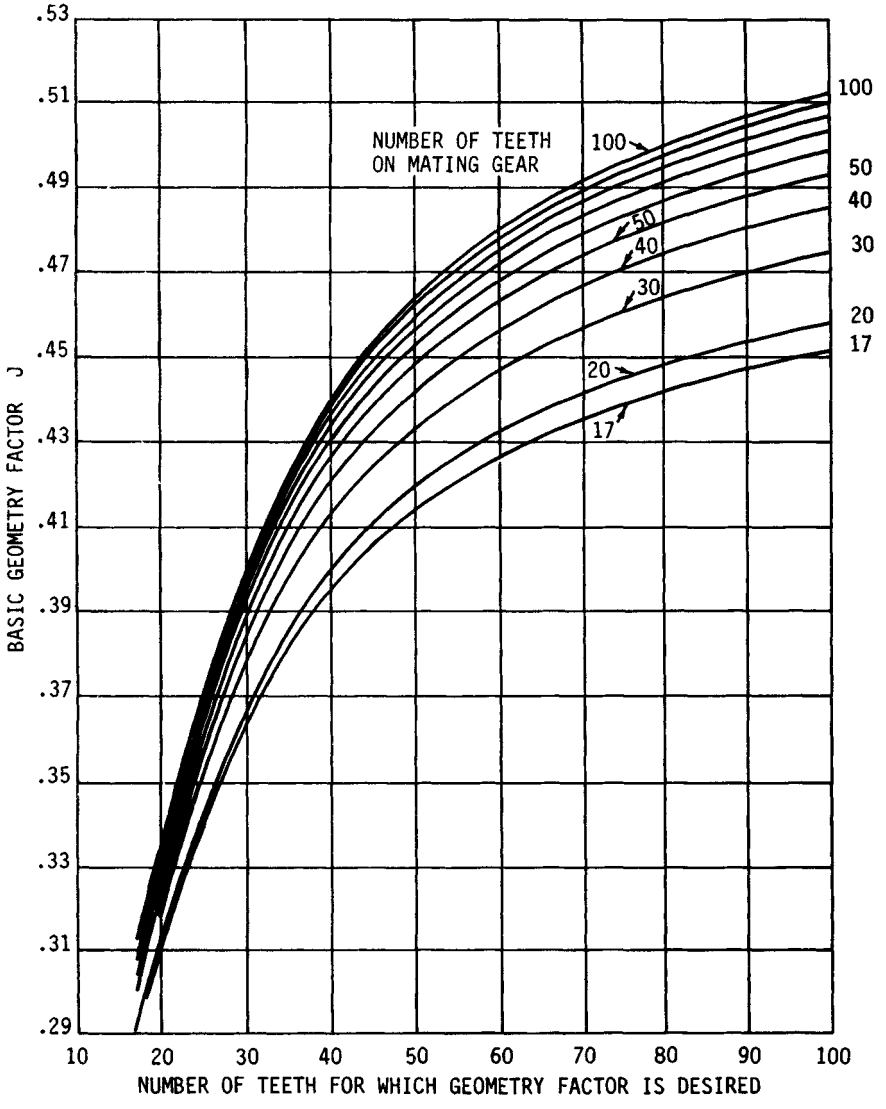

FIGURE 35.11 Basic geometry factors for 20° spur teeth; $\phi_N = 20°$, $a = 1.00$, $b = 1.35$, $r_T = 0.42$, $\Delta t = 0$.

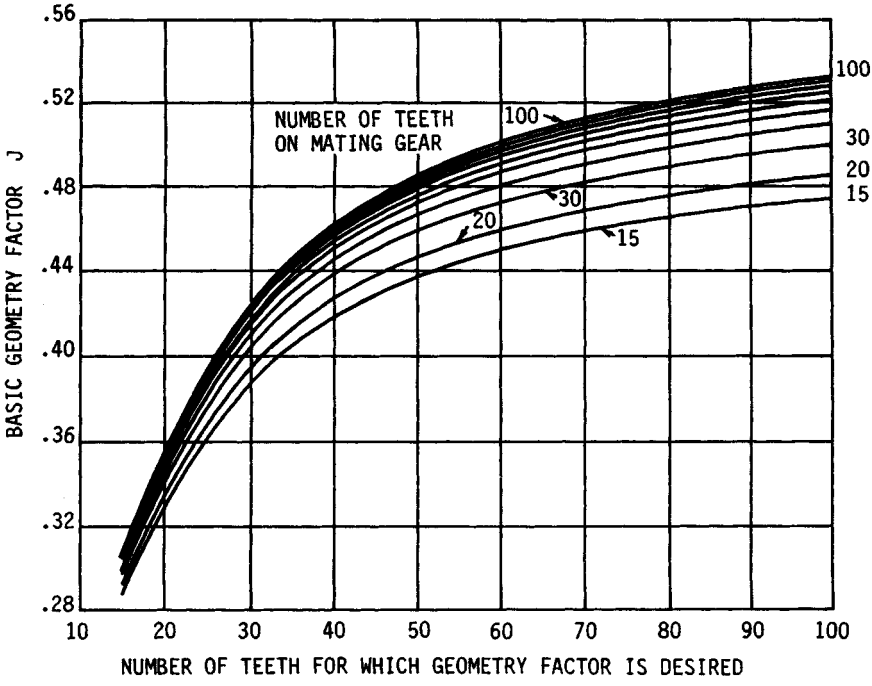

FIGURE 35.12 Basic geometry factors for 22½° spur teeth; $\phi_N = 22½°$, $a = 1.00$, $b = 1.35$, $r_T = 0.34$, $\Delta t = 0$.

at least 2.0 for other cutting-tool configurations, are shown in Figs. 35.26 through 35.36.† For these figures,

$$m_N = \frac{P_N}{0.95Z} \tag{35.48}$$

where the value of Z is for an element of indicated number of teeth and a 75-tooth mate. Also, the normal tooth thicknesses of pinion and gear teeth are each reduced 0.024 in, to provide 0.048 in of total backlash corresponding to a normal diametral pitch of unity. Note that these charts are limited to standard addendum, dedendum, and tooth thickness designs.

If the face-contact ratio is less than 2.0, the geometry factor must be calculated in accordance with Eq. (35.46); thus, it will be necessary to define Y and K_f. The definition of Y may be accomplished either by graphical layout or by a numerical iteration procedure. Since this Handbook is likely to be used by the machine designer with an occasional need for gear analysis, rather than by the gear specialist, we present the direct graphical technique. Readers interested in preparing computer codes or calculator routines might wish to consult Ref. [35.6].

The following graphical procedure is abstracted directly from Ref. [35.1] with permission of the publisher, as noted earlier. The Y factor is calculated with the aid

† These figures are extracted from AGMA 218.01 with the permission of the AGMA.

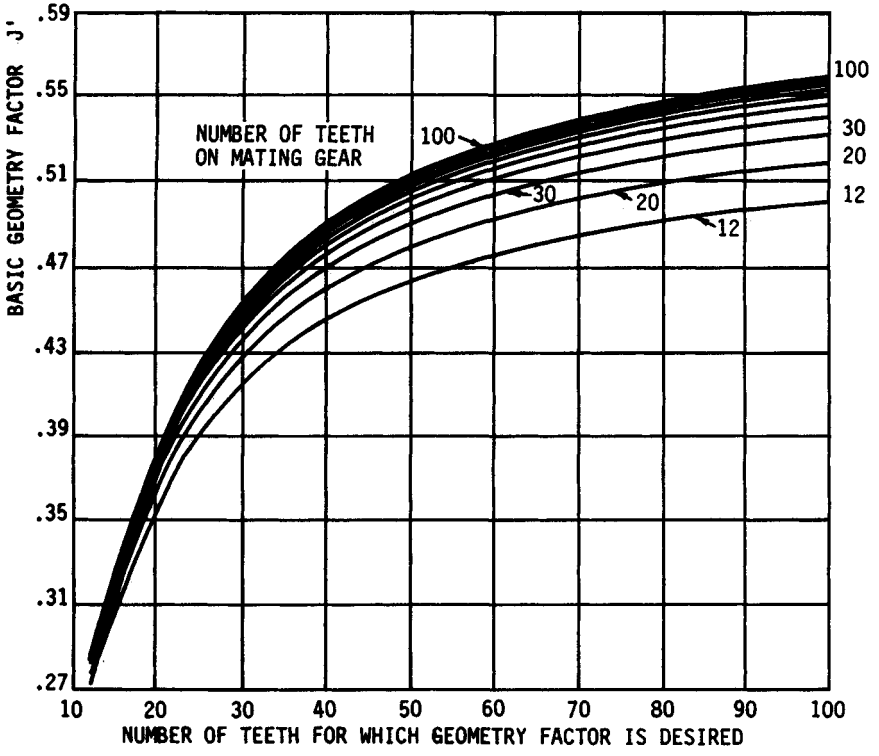

FIGURE 35.13 Basic geometry factors for 25° spur teeth; $\phi_N = 25°$, $a = 1.00$, $b = 1.35$, $r_T = 0.24$, $\Delta t = 0$.

of dimensions obtained from an accurate layout of the tooth profile in the normal plane at a scale of 1 normal diametral pitch. Actually, any scale can be used, but the use of 1 normal diametral pitch is most convenient. Depending on the face-contact ratio, the load is considered to be applied at the highest point of single-tooth contact (HPSTC), Fig. 35.37, or at the tooth tip, Fig. 35.37. The equation is

$$Y = \frac{K_\psi P_s}{[\cos(\phi_L)/\cos(\phi_{No})][(1.5/uC_h) - \tan(\phi_L)/t]} \tag{35.49}$$

The terms in Eq. (35.49) are defined as follows:

K_ψ = helix-angle factor
ϕ_{No} = normal operating pressure angle [Eq. (35.14)]
ϕ_L = load angle
C_h = helical factor
t = tooth thickness from layout, in
u = radial distance from layout, in
P_s = normal diametral pitch of layout (scale pitch), usually 1.0 in^{-1}

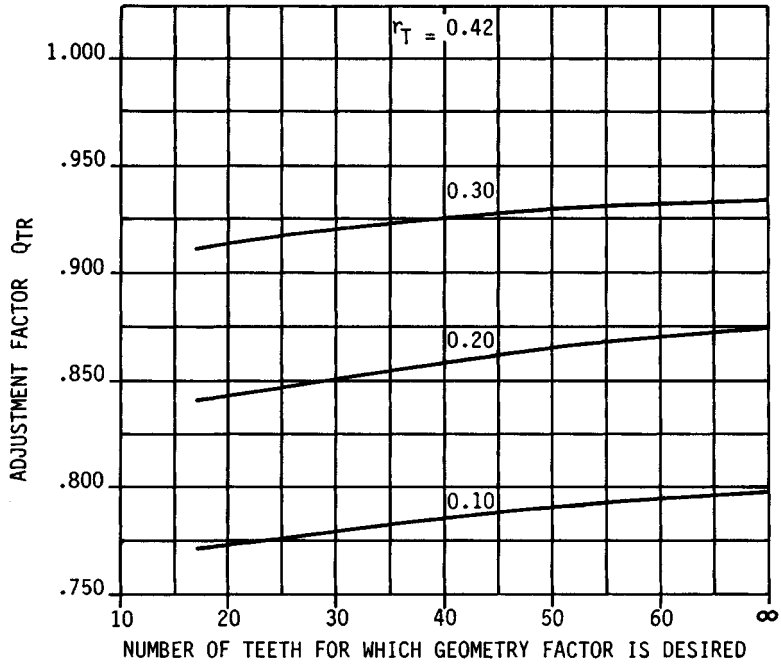

FIGURE 35.14 Tool-tip radius adjustment factor for 20° spur teeth. Tool-tip radius = r_T for a 1-diametral-pitch gear.

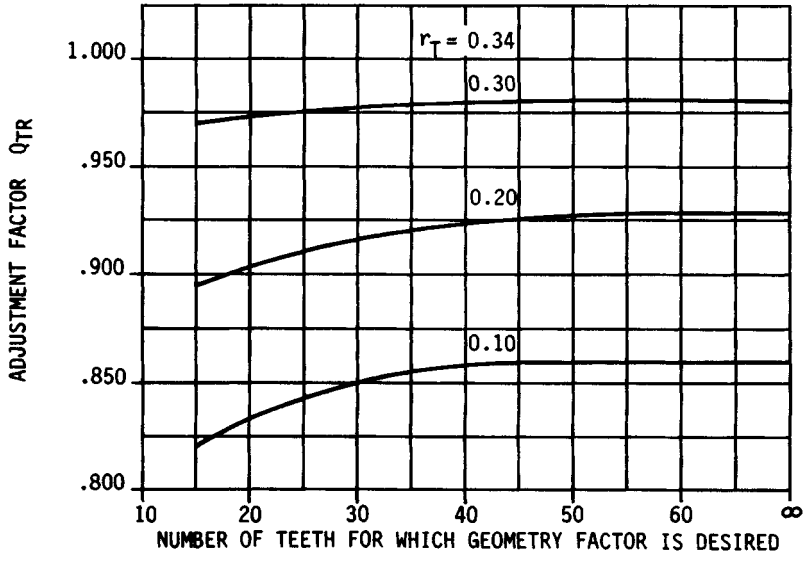

FIGURE 35.15 Tool-tip radius adjustment factor for 22½° spur teeth. Tool-tip radius = r_T for a 1-diametral-pitch gear.

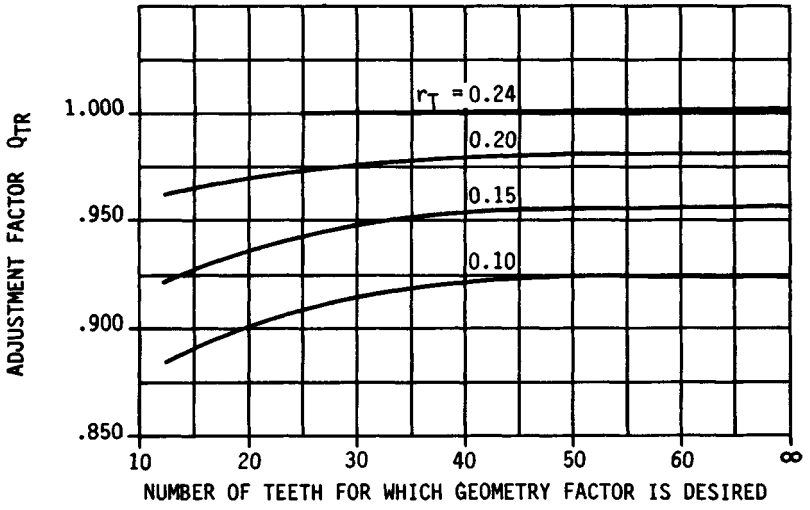

FIGURE 35.16 Tool-tip radius adjustment factor for 25° spur teeth. Tool-tip radius = r_T for a 1-diametral-pitch gear.

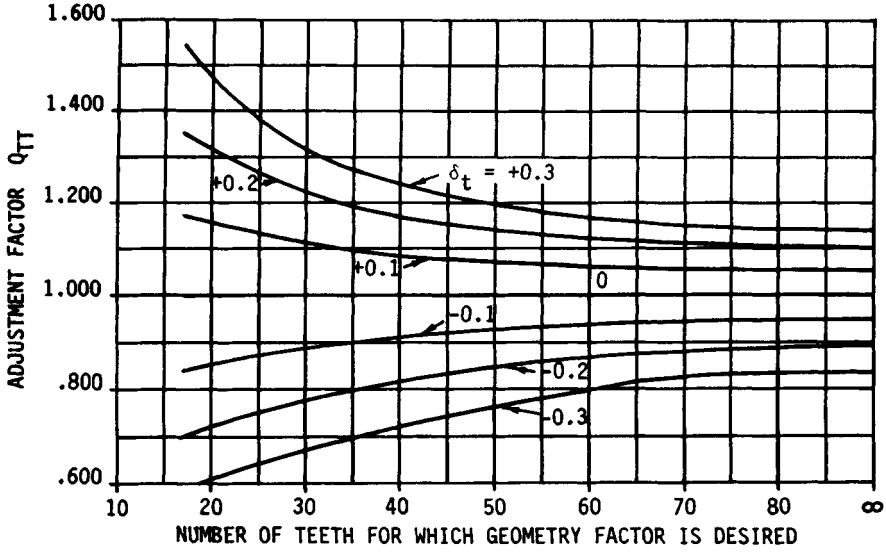

FIGURE 35.17 Tooth thickness adjustment factor Q_{TT} for 20° spur teeth. Tooth thickness modification = δ_t for 1-diametral-pitch gears.

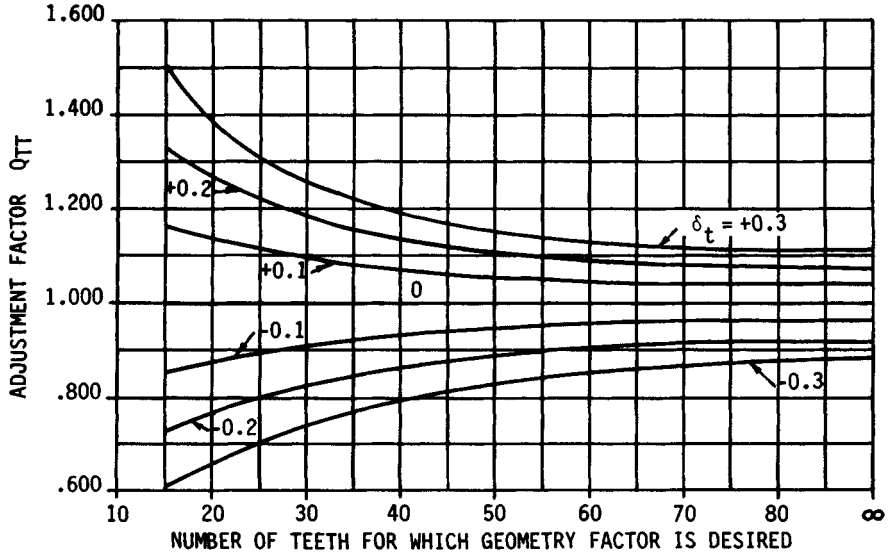

FIGURE 35.18 Tooth thickness adjustment factor Q_{TT} for 22½° spur teeth. Tooth thickness modification = δ_t for 1-diametral-pitch gears.

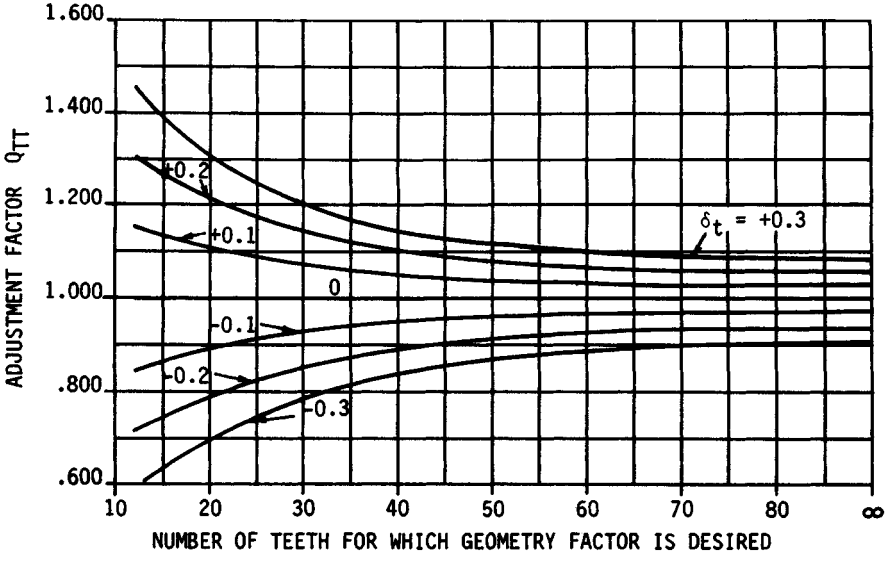

FIGURE 35.19 Tooth thickness adjustment factor Q_{TT} for 25° spur teeth. Tooth thickness modification = δ_t for 1-diametral-pitch gears.

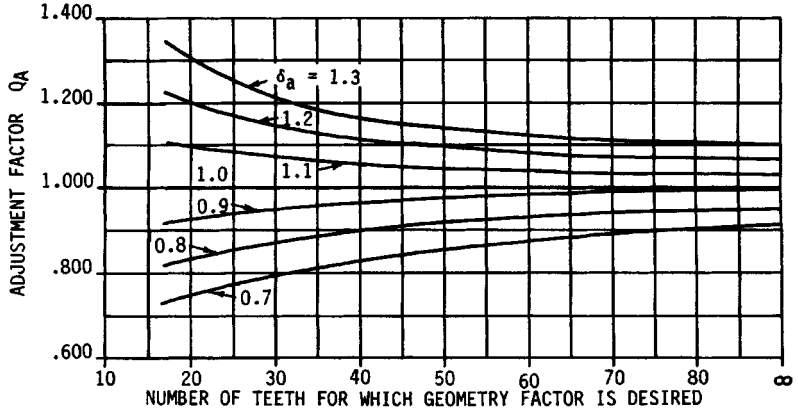

FIGURE 35.20 Addendum adjustment factor Q_A for 20° spur teeth. Addendum factor modification = δ_a for 1-diametral-pitch gears.

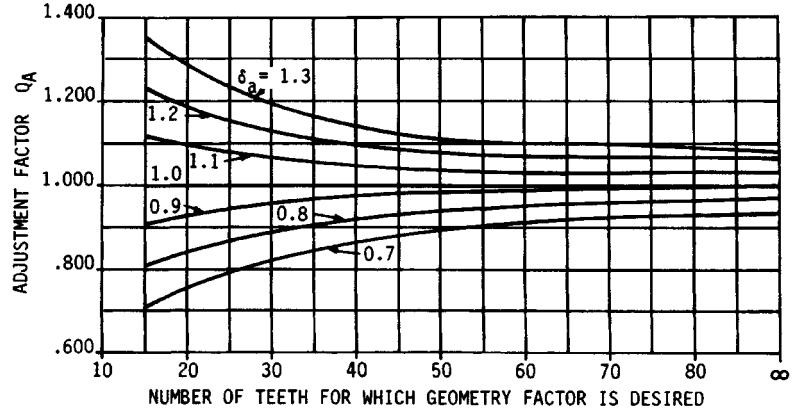

FIGURE 35.21 Addendum adjustment factor Q_A for 22½° spur teeth. Addendum factor modification = δ_a for 1-diametral-pitch gears.

To make the Y factor layout for a helical gear, an equivalent normal-plane gear tooth must be created, as follows:

$$N_e = \frac{N_P}{\cos^3 \psi} \tag{35.50}$$

$$d_c = \frac{dP_{nd}}{\cos^2 \psi} \tag{35.51}$$

$$d_{be} = d_e \cos \phi_n = N_e \cos \phi_c \tag{35.52}$$

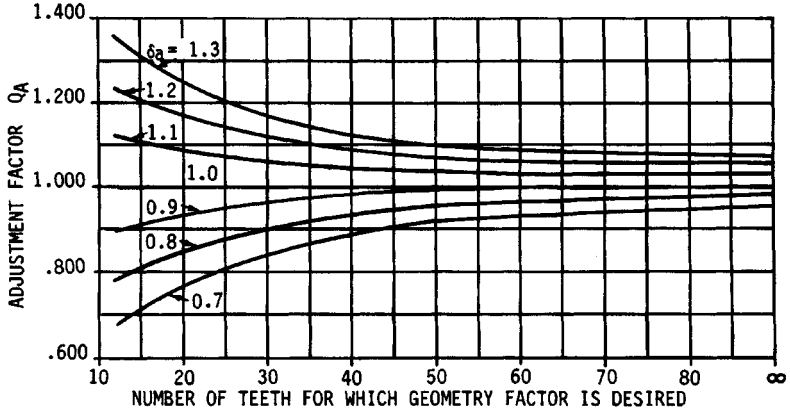

FIGURE 35.22 Addendum adjustment factor Q_A for 25° spur teeth. Addendum factor modification = δ_a for 1-diametral-pitch gears.

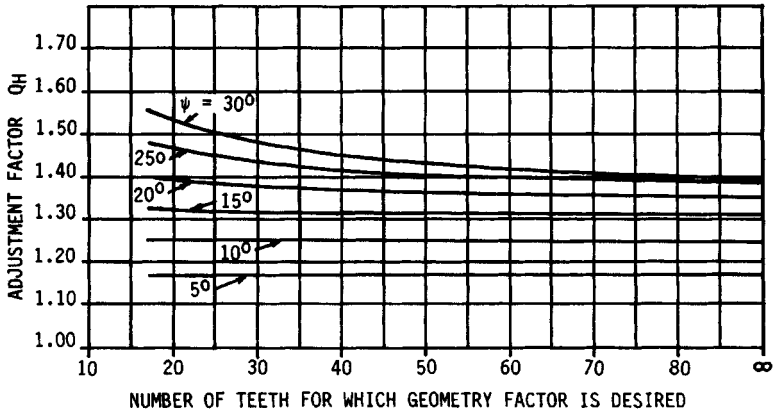

FIGURE 35.23 Helix-angle adjustment factor Q_H for $\phi_N = 20°$.

$$a = \frac{d_o - d}{2} P_{nd} \tag{35.53}$$

$$b = \frac{d - d_R}{2} P_{nd} \tag{35.54}$$

$$d_{oe} = d_e + 2a \tag{35.55}$$

$$d_{Re} = d_e - 2b \tag{35.56}$$

$$r_1 = \frac{(b - r_{Te})^2}{R_o + b - r_{Te}} \tag{35.57}$$

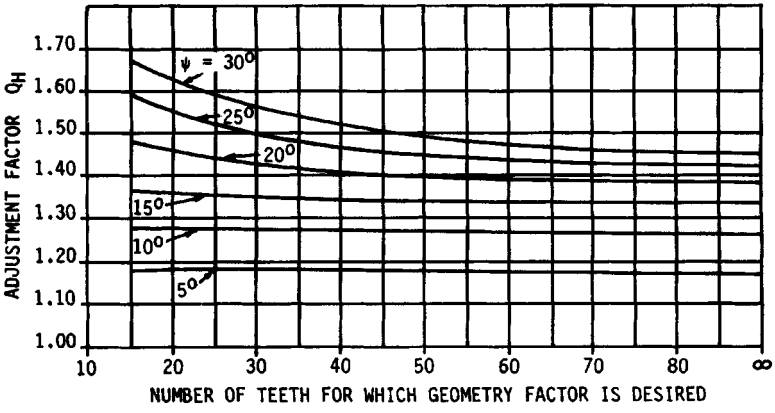

FIGURE 35.24 Helix-angle adjustment factor Q_H for $\phi_N = 22\frac{1}{2}°$.

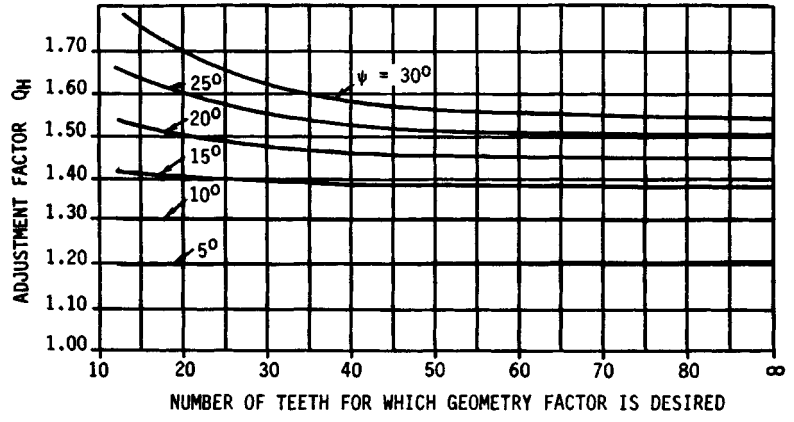

FIGURE 35.25 Helix-angle adjustment factor Q_H for $\phi_N = 25°$.

$$r_f = r_1 + r_{Te} \tag{35.58}$$

$$r_{Te} = r_T P_{nd} \tag{35.59}$$

For a hob or rack-shaped cutting tool,

$$R_o = \frac{d_{se}}{2} \tag{35.60}$$

For a pinion-shaped cutting tool,

$$R_o = \frac{d_{se} D_c P_{nd}}{2(d_{se} + D_c P_{nd})} \tag{35.61}$$

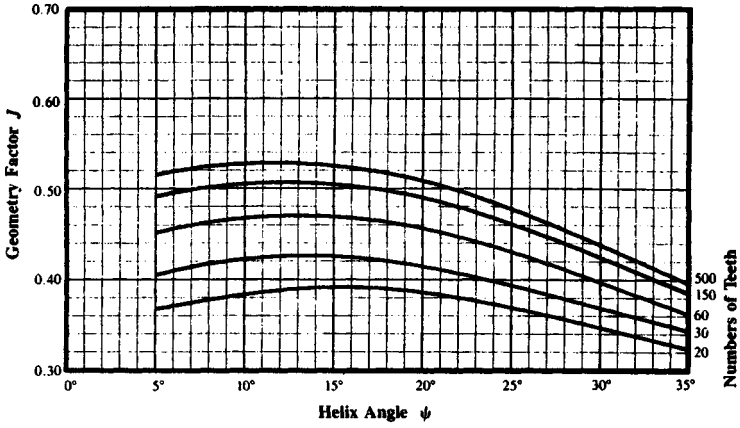

FIGURE 35.26 Geometry factor J for a 14½° normal-pressure-angle helical gear. These factors are for a standard addendum finishing hob as the final machining operation. See Fig. 35.27*a*. *(From AGMA 218.01.)*

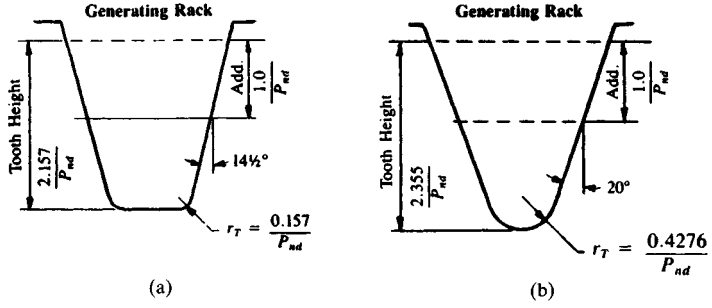

FIGURE 35.27 Generating racks. (*a*) For teeth of Fig. 35.26; (*b*) for teeth of Fig. 35.29. *(From AGMA 218.01.)*

$$D_e = \frac{DP_{nd}}{\cos^2 \psi} \tag{35.62}$$

$$A = \frac{D_o - D}{2} P_{nd} \tag{35.63}$$

$$D_{oe} = D_e + 2A \tag{35.64}$$

$$D_{be} = D_e \cos \phi_n \tag{35.65}$$

$$d_{se} = \frac{N_e}{P_s} \tag{35.66}$$

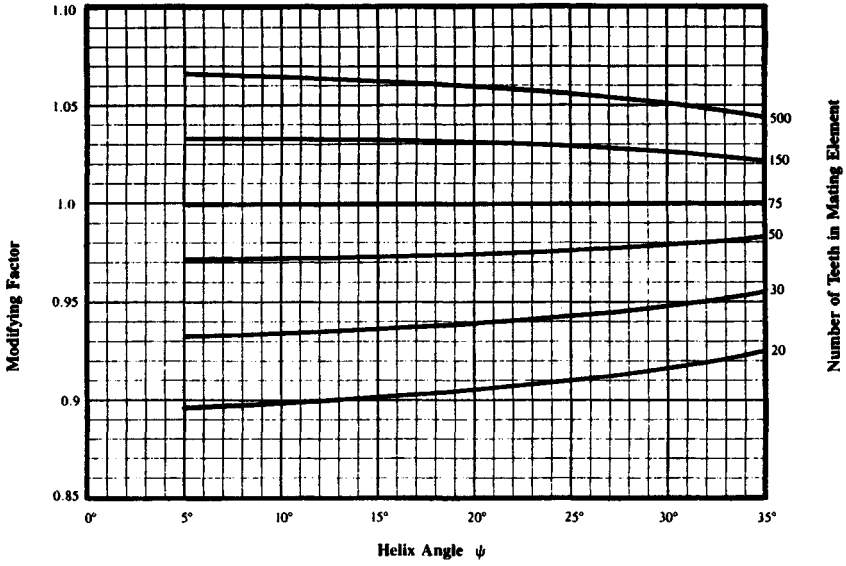

FIGURE 35.28 *J* factor multipliers for 14½° normal-pressure-angle helical gear. These factors can be applied to the *J* factor when other than 75 teeth are used in the mating element. *(From AGMA 218.01.)*

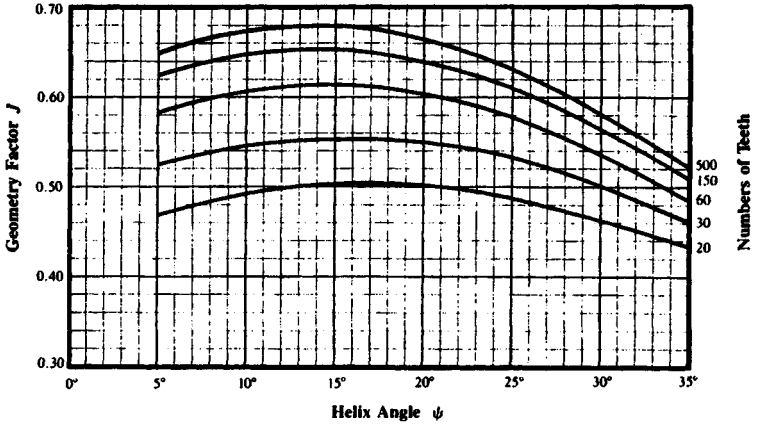

FIGURE 35.29 Geometry factor *J* for a 20° normal-pressure-angle helical gear. These factors are for standard addendum teeth cut with a full-fillet hob. See Fig. 35.27*b*. *(From AGMA 218.01.)*

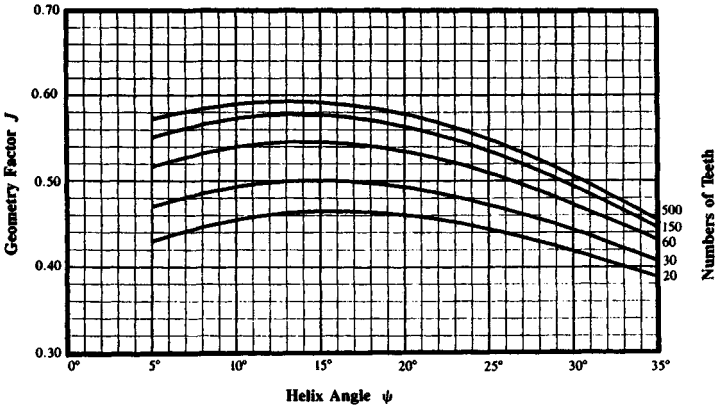

FIGURE 35.30 Geometry factor J for a 20° normal-pressure-angle helical gear. These factors are for standard addendum teeth cut with a finishing hob as the final machining operation. See Fig. 35.31*a*. *(From AGMA 218.01.)*

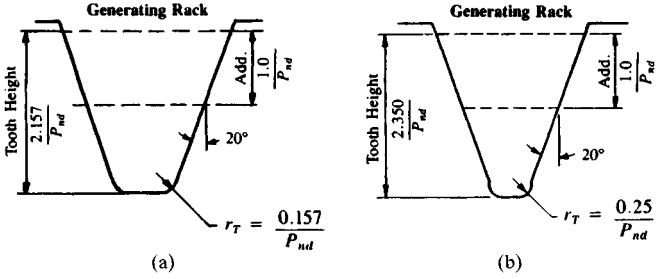

FIGURE 35.31 Generating racks. (*a*) For teeth of Fig. 35.30; (*b*) for teeth of Fig. 35.32. *(From AGMA 218.01.)*

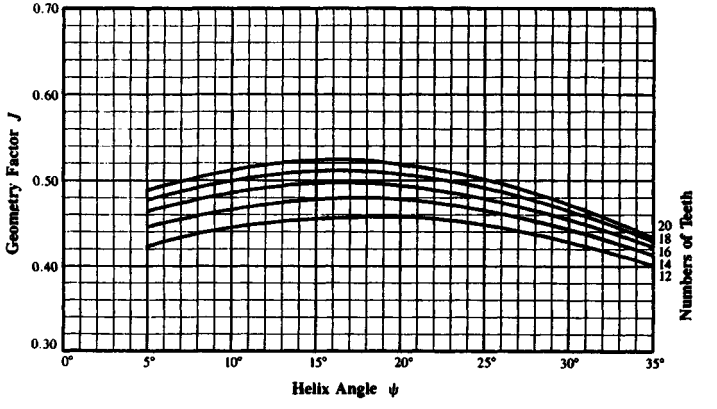

FIGURE 35.32 Geometry factor J for 20° normal-pressure-angle helical gear. These factors are for long-addendum (125 percent of standard) shaved teeth cut with a preshave hob. See Fig. 35.31*b*. *(From AGMA 218.01.)*

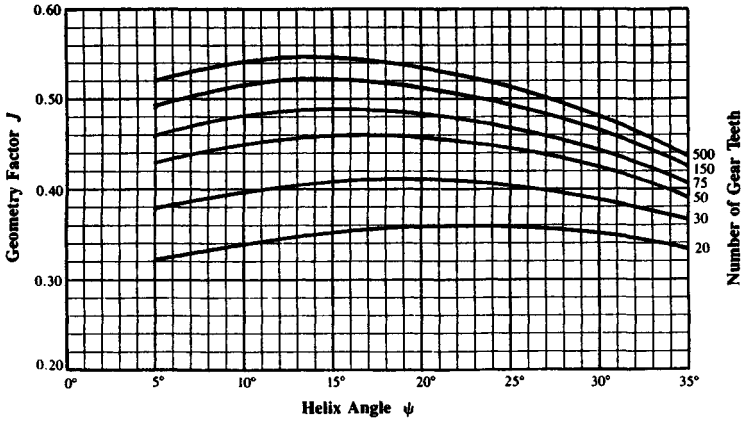

FIGURE 35.33 Geometry factor J for 20° normal-pressure-angle helical gear. These factors are for short-addendum teeth (75 percent of standard) cut with a preshave hob. See Fig. 35.34. *(From AGMA 218.01.)*

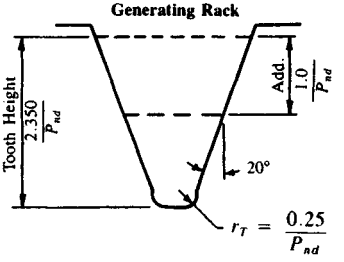

FIGURE 35.34 Generating rack for teeth of Fig. 35.33. *(From AGMA 218.01.)*

where N_e = equivalent number of pinion teeth
d_{se} = equivalent generating pitch diameter, in
d_R = root diameter for actual number of teeth and generated pitch, in
d_{Re} = equivalent root diameter for equivalent number of teeth, in
d_{be} = equivalent base diameter for equivalent number of teeth, in
d_e = equivalent operating pitch diameter for equivalent number of teeth, in
d_{oe} = equivalent outside diameter for equivalent number of teeth, in
a = operating addendum of pinion at 1 normal diametral pitch, in
b = operating dedendum of pinion at 1 normal diametral pitch, in
r_f = minimum fillet radius at root circle of layout, in
r_T = edge radius of cutting tool, in
r_{Te} = equivalent edge radius of cutting tool, in
R_o = relative radius of curvature of pitch circle of pinion and pitch line or circle of cutting tool, in
D_c = pitch diameter of pinion-shaped cutting tool, in
D_e = equivalent operating pitch diameter of mating gear for equivalent number of teeth, in

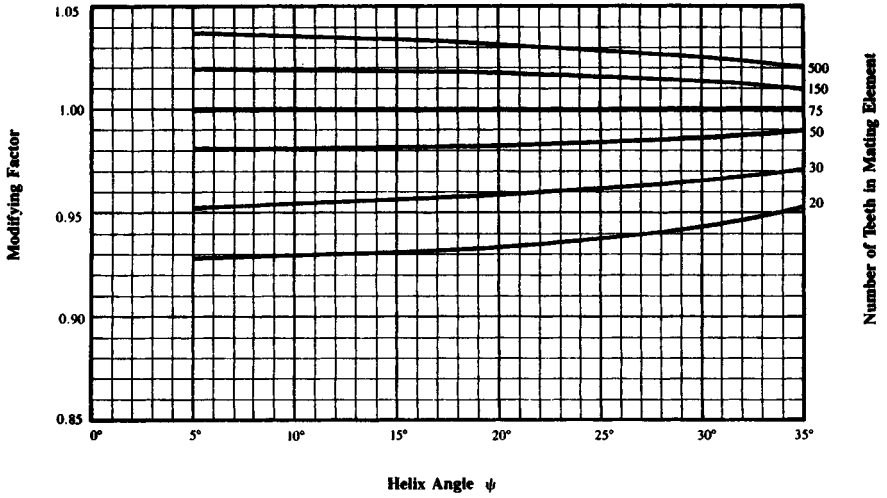

FIGURE 35.35 *J* factor multipliers for 20° normal-pressure-angle helical gears. These factors can be applied to the *J* factor when other than 75 teeth are used in the mating element. *(From Ref. [35.1].)*

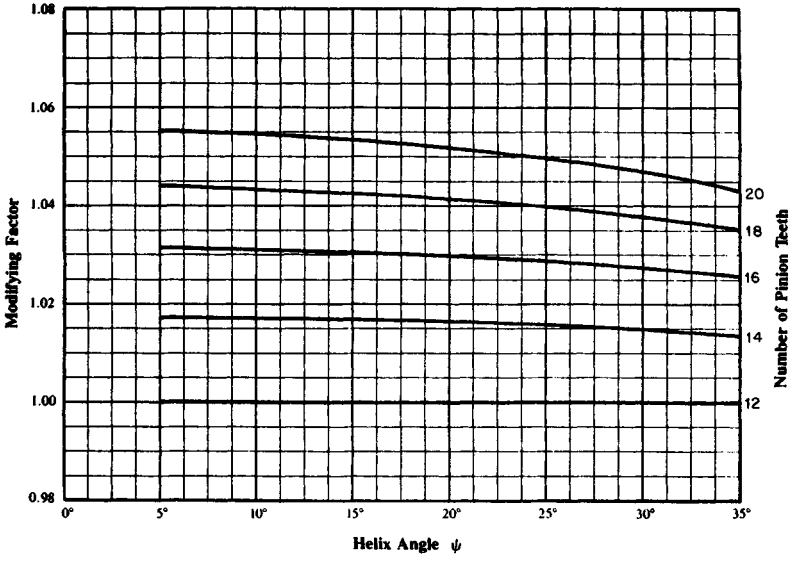

FIGURE 35.36 *J* factor multipliers for 20° normal-pressure-angle helical gears with short addendum (75 percent of standard). These factors can be applied to the *J* factor when other than 75 teeth are used in the mating element. *(From Ref. [35.1].)*

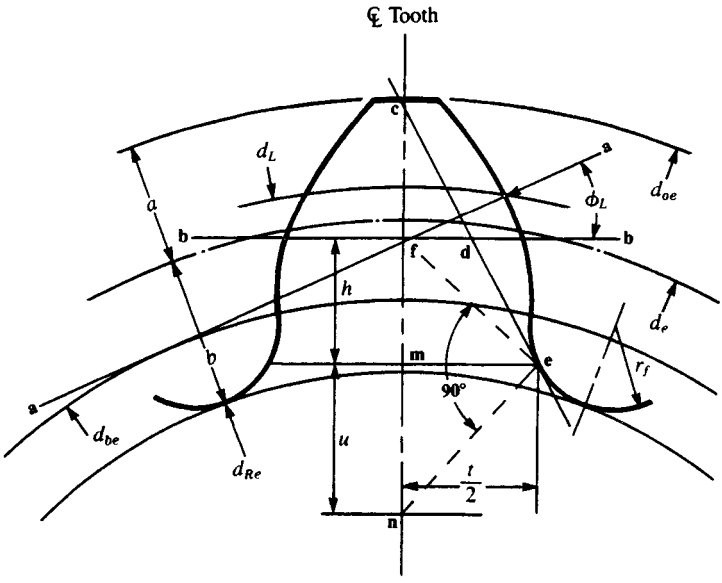

FIGURE 35.37 Tooth form factor with load at highest point of single-tooth contact (HPSTC) shown in the normal plane through the pitch point. Note that r_f occurs at the point where the trochoid meets the root radius. *(From Ref. [35.1].)*

D_{oe} = equivalent outside diameter of mating gear for equivalent number of teeth, in
D_{be} = equivalent base diameter of mating gear for equivalent number of teeth, in
A = operating addendum of mating gear at 1 normal diametral pitch, in

The dimensions defined by Eqs. (35.50) through (35.66) are then used to make a tooth-stress layout, as shown in either Fig. 35.37 or 35.38 as required by the face-contact ratio. That is, helical gears with low face-contact ratio ($m_F \leq 1.0$) are assumed to be loaded at the highest point of single-tooth contact; normal helical gears ($m_F > 1.0$) use tip loading, and the C_h factor compensates for the actual loading on the oblique line.

To find Y from the above data, a graphical construction, as follows, is required. For low-contact-ratio helical gears (with $m_F \leq 1.0$), using Fig. 35.37, draw a line $\overline{aa}$ through point p, the intersection of diameter d_L with the profile, and tangent to the base diameter d_{be}:

$$d_L = 2\left\{\left[\sqrt{\left(\frac{d_e}{2}\right)^2 - \left(\frac{d_{be}}{2}\right)^2} + Z_d\right]^2 + \left(\frac{d_{be}}{2}\right)^2\right\}^{1/2} \tag{35.67}$$

where Z_d = distance on line of action from highest point of single-tooth contact to pinion operating pitch circle, in inches, and so

$$Z_d = \pi \cos \phi_c - Z_e \tag{35.68}$$

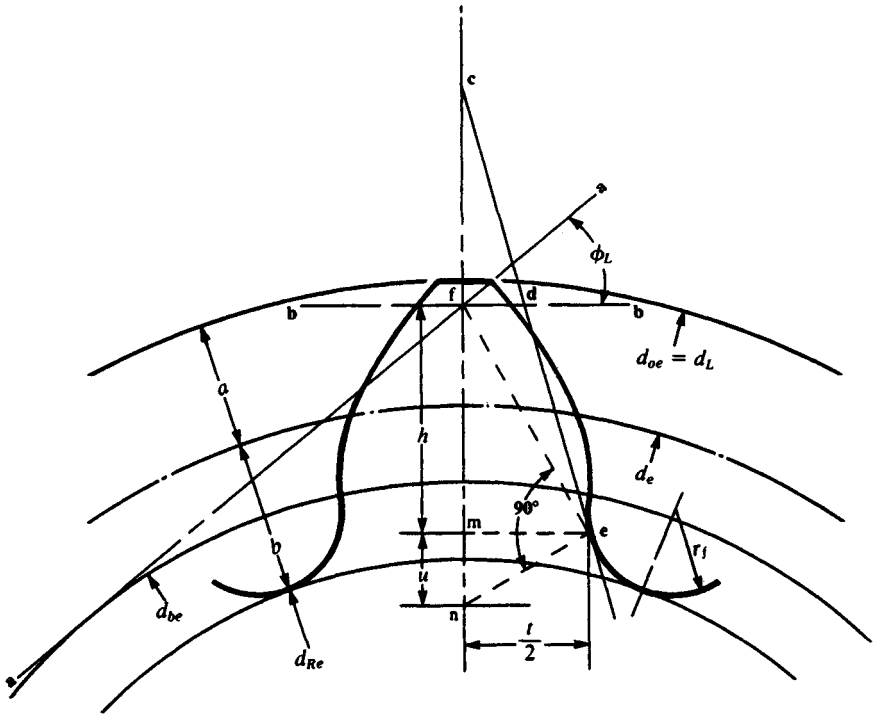

FIGURE 35.38 Tooth form factor layout with load at tooth tip; shown in normal plane through the pitch point. *(From Ref. [35.1].)*

Letting Z_e = distance on line of action from gear outside diameter to pinion operating pitch circle, in inches, we have

$$Z_e = \sqrt{\left(\frac{D_{oe}}{2}\right)^2 - \left(\frac{D_{be}}{2}\right)^2} - \sqrt{\left(\frac{D_e}{2}\right)^2 - \left(\frac{D_{be}}{2}\right)^2} \tag{35.69}$$

For normal helical gears with $m_F > 1.0$, using Fig. 35.38, we find $D_L = d_{oe}$. Draw a line $\overline{aa}$ through point p, the tip of the tooth profile, and tangent to the base diameter d_{be}. Continue the layout for all gear types as follows:

Through point f, draw a line $\overline{bb}$ perpendicular to the tooth centerline. The included angle between lines $\overline{aa}$ and $\overline{bb}$ is load angle ϕ_L.

Draw line $\overline{cde}$ tangent to the tooth fillet radius r_f at e, intersecting line $\overline{bb}$ at d and the tooth centerline at c so that $\overline{cd} = \overline{de}$.

Draw line $\overline{fe}$.

Through point e, draw a line perpendicular to $\overline{fe}$, intersecting the tooth centerline at n.

Through point e, draw a line $\overline{me}$ perpendicular to the tooth centerline.

Measure the following in inches from the tooth layout:

$$\overline{mn} = u \qquad \overline{me} = \frac{t}{2}$$

and

$$\overline{mf} = h \qquad \text{(required for calculating } K_f\text{)}$$

The helix-angle factor K_ψ is set equal to unity for helical gears with $m_F \leq 1.0$, but for helical gears with $m_F > 1.0$, it is given by

$$K_\psi = \cos \psi_o \cos \psi \tag{35.70}$$

where ψ_o = helix angle at operating pitch diameter [from Eq. (35.13)] and ψ = helix angle at standard pitch diameter.

The helical factor C_h is the ratio of the root bending moment produced by the same intensity of loading applied along the actual oblique contact line (Fig. 35.39). If the face width of one gear is substantially larger than that of its mate, then full buttressing may exist on the wider face gear. If one face is wider than its mate by at least one addendum on *both* sides, then the value of C_h defined below may be increased by 10 percent only. The helical factor is given by either Eq. (35.71) for low-contact-ratio helical gears ($m_F \leq 1.0$) or Eq. (35.72) for normal-contact-ratio ($m_F > 1.0$) helicals. These equations are valid only for helix angles up to 30°:

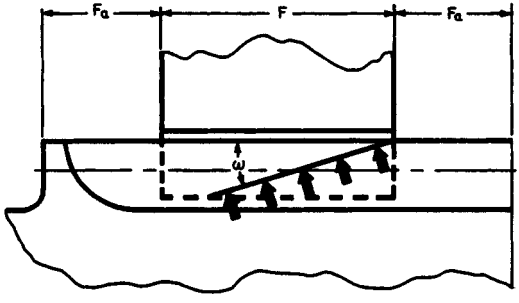

FIGURE 35.39 Oblique contact line. Full buttressing exists when $F_a \geq$ one addendum.

$$C_h = 1.0 \tag{35.71}$$

$$C_h = \frac{1.0}{1 - [(\omega/100)\,(1 - \omega/100)]^{1/2}} \tag{35.72}$$

where $\omega = \tan^{-1}(\tan \psi_o \sin \phi_{No})$ = inclination angle, deg
ψ_o = helix angle at operating pitch diameter, deg [Eq. (35.13)]
ϕ_{No} = operating normal pressure angle, deg [Eq. (35.14)]

The tooth form factor Y may now be calculated from Eq. (35.49).

The stress correction factor is the last item which must be calculated prior to finding a value for the bending geometry factor J. Based on photoelastic studies by Dolan and Broghamer, the empirical relations shown in Eqs. (35.73) through (35.76) were developed:

$$K_f = H + \left(\frac{t}{r_f}\right)^L \left(\frac{t}{h}\right)^m \tag{35.73}$$

$$H = 0.18 - 0.008(\phi_{No} - 20) \tag{35.74}$$

$$L = H - 0.03 \tag{35.75}$$

$$m = 0.45 + 0.010(\phi_{No} - 20) \tag{35.76}$$

Elastic Coefficient $\mathbf{C_p}$. This factor accounts for the elastic properties of various gear materials. It is given by Eq. (35.77). Table 35.4 provides values directly for C_p for various material combinations, for which Poisson's ratio is 0.30.

TABLE 35.4 Values of Elastic Coefficient C_p for Helical Gears with Nonlocalized Contact and for $\upsilon = 0.30$

Pinion material	Gear material					
	Steel	Malleable iron	Nodular iron	Cast iron	Aluminum bronze	Tin bronze
Steel, E = 30†	2300	2180	2160	2100	1950	1900
Malleable iron, E = 25	2180	2090	2070	2020	1900	1850
Nodular iron, E = 24	2160	2070	2050	2000	1880	1830
Cast iron, E = 22	2100	2020	2000	1960	1850	1800
Aluminum bronze, E = 17.5	1950	1900	1880	1850	1750	1700
Tin bronze, E = 16	1900	1850	1830	1800	1700	1650

†Modulus of elasticity E is in megapounds per square inch (Mpsi).

$$C_p = \left\{ \frac{1}{\pi[(1 - \nu_P^2)/E_P + (1 - \nu_G^2)/E_G]} \right\}^{1/2} \tag{35.77}$$

where ν_P, ν_G = Poisson's ratio for pinion and gear, respectively
E_P, E_G = modulus of elasticity for pinion and gear, respectively

Allowable Stresses $\mathbf{s_{ac}}$ ***and*** $\mathbf{s_{at}}$. The allowable stresses depend on many factors, such as chemical composition, mechanical properties, residual stresses, hardness, heat treatment, and cleanliness. As a guide, the allowable stresses for helical gears may be obtained from Tables 35.5 and 35.6 or Figs. 35.40 and 35.41. Where a range of values is shown, the lowest values are used for general design. The upper values may be used only when the designer has certified that

1. High-quality material is used.
2. Section size and design allow maximum response to heat treatment.
3. Proper quality control is effected by adequate inspection.
4. Operating experience justifies their use.

Surface-hardened gear teeth require adequate case depth to resist the subsurface shear stresses developed by tooth contact loads and the tooth root fillet tensile stresses. But depths must not be so great as to result in brittle teeth tips and high residual tensile stress in the core.

TABLE 35.5 Allowable Bending Stress Numbers s_{at} and Contact Stress Numbers s_{ac} for a Variety of Materials

AGMA class	Commercial designation	Heat treatment	Minimum hardness		s_{at}, kpsi	s_{ac}, kpsi
			Surface	Core		
		Steel				
A-1 through A-5		Through-hardened and tempered (Fig. 35-40)	180 H_B and less		25–33	85–95
			240 H_B		31–41	105–115
			300 H_B		36–47	120–135
			360 H_B		40–52	145–160
			400 H_B		42–56	155–170
		Flame- or induction-hardened† with type A pattern (Fig. 35-45)	50–54 R_C		45–55	170–190
		Flame- or induction-hardened with type B pattern (Fig. 35-45)			22	
		Carburized† and case-hardened†	55 R_C		55–65	180–200
			60 R_C		55–70	200–225
	AISI 4140	Nitrided†‡	48 R_C	300 H_B	35–45	155–180
	AISI 4340	Nitrided†‡	46 R_C	300 H_B	36–47	150–175
	Nitralloy 135M	Nitrided†‡	60 R_C	300 H_B	38–48	170–195
	$2\frac{1}{2}$% chrome	Nitrided†‡	54–60 R_C	350 H_B	55–65	155–216

Cast iron						
20		As cast			5	50–60
30		As cast	175 H_B		8.5	65–75
40		As cast	200 H_B		13	75–85
Nodular (ductile) iron						
A-7-a	60-40-18	Annealed,	140 H_B		22–33	77–92
A-7-c	80-55-06	quenched, and	180 H_B		22–33	77–92
A-7-d	100-70-03	tempered	230 H_B		27–40	92–112
A-7-e	120-90-02		270 H_B		31–44	103–126
Malleable iron (pearlitic)						
A-8-c	45007		165 H_B		10	72
A-8-e	50005		180 H_B		13	78
A-8-f	53007		195 H_B		16	83
A-8-i	80002		240 H_B		21	94
Bronze						
Bronze 2	AGMA 2C	Sand-cast Sand-cast	Min. tensile strength 40 kpsi		5.7	30
Al/Br 3	ASTM B-148-52 Alloy 9C	Heat-treated	Min. tensile strength 90 kpsi		23.6	65

†The range of allowable stress numbers indicated corresponds to grade 1 and grade 2 steels. See tables 14-6 and 14-9 to 14-11 of source.

‡The overload capacity of nitrided gears is low, since the shape of the effective SN curve is flat. The sensitivity to shock should be investigated before proceeding with the design.

SOURCE: **Ref. [35.1].**

TABLE 35.6 Reliability Factors K_R and C_R

Factor, K_R or C_R	Probabilities, %	
	Success	Failure
1.50	99.99	0.01
1.25	99.90	0.10
1.00	99.00	1.00
0.85	90.00	10.00

The effective case depth for carburized and induction-hardened gears is defined as the depth below the surface at which the Rockwell C hardness has dropped to 50 R_C or to 5 points below the surface hardness, whichever is lower.

The values and ranges shown in Fig. 35.42 have had a long history of successful use for carburized gears and can be used as guides. For gearing in which maximum performance is required, detailed studies must be made of the application, loading, and manufacturing procedures, to obtain desirable gradients of both hardness and internal stress. Furthermore, the method of measuring the case, as well as the allowable tolerance in case depth, should be a matter of agreement between the customer and the manufacturer.

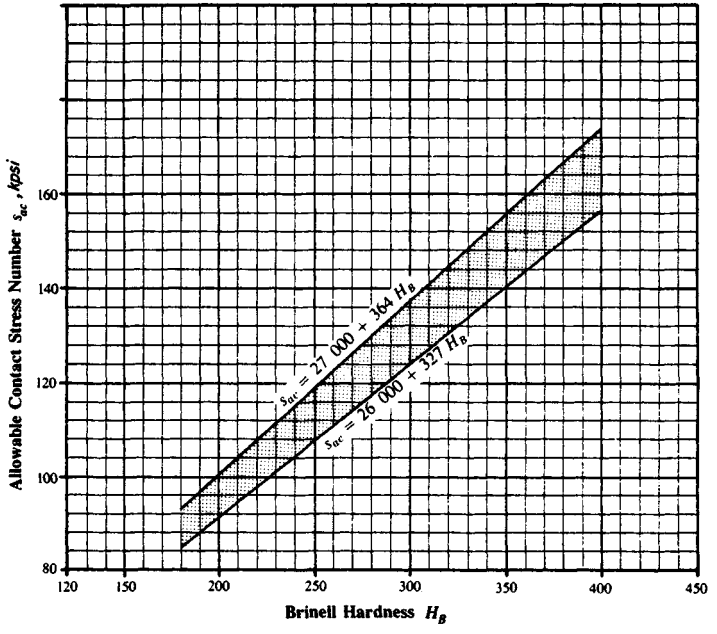

FIGURE 35.40 Allowable contact stress number s_{ac} for steel gears. Lower curve is maximum for grade 1 and upper curve is maximum for grade 2. *(From Ref. [35.1].)*

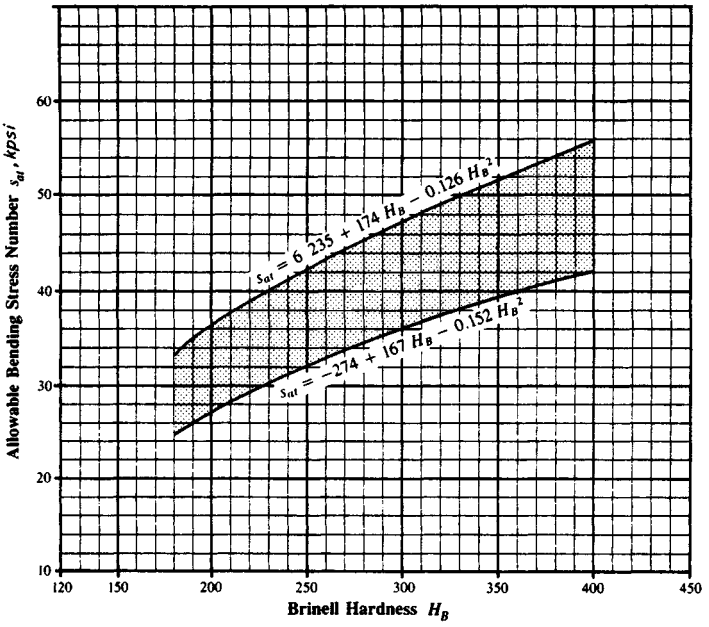

FIGURE 35.41 Allowable bending stress number s_{at} for steel gears. Lower curve is maximum for grade 1 and upper curve is maximum for grade 2. *(From Ref. [35.1].)*

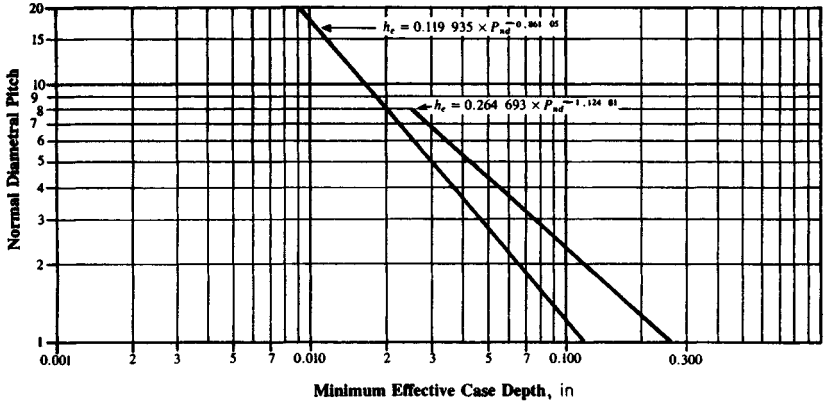

FIGURE 35.42 Effective case depth h_e for carburized gears based on normal diametral pitch. The effective case depth is defined as the depth of case which has a minimum hardness of 50 R_C. The total case depth to core carbon is about $1.5h_e$. The values and ranges shown on the case depth curves are to be used as guides. For gearing in which maximum performance is required, detailed studies must be made of the application, loading, and manufacturing procedures to obtain desirable gradients of both hardness and internal stress. Furthermore, the method of measuring the case as well as the allowable tolerance in case depth should be a matter of agreement between the customer and the manufacturer. *(From Ref. [35.1].)*

A guide for minimum effective case depth h_e at the pitch line for carburized and induction-hardened teeth, based on the depth of maximum shear from contact loading, is given by

$$h_e = \frac{C_G s_c d \sin \phi_o}{U_H \cos \psi_b} \tag{35.78}$$

where h_e = minimum effective case depth in inches and U_H = hardening process factor in pounds per square inch. In Eq. (35.78), $U_H = 6.4 \times 10^6$ psi for carburized teeth and 4.4×10^6 psi for tooth-to-tooth induction-hardened teeth.

You should take care when using Eq. (35.78) that adequate case depths prevail at the tooth root fillet, and that tooth tips are not overhardened and brittle. A suggested value of maximum effective case depth $h_{e,\max}$ at the pitch line is

$$h_{e,\max} = \frac{0.4}{P_d} \qquad \text{or} \qquad h_{e,\max} = 0.56 t_o \tag{35.79}$$

where $h_{e,\max}$ = suggested maximum effective case depth in inches and t_o = normal tooth thickness at top land of gear in question, in inches.

For nitrided gears, case depth is specified as total case depth h_c, and h_c is defined as the depth below the surface at which the hardness has dropped to 110 percent of the core hardness.

For gearing requiring maximum performance, especially large sizes, coarse pitches, and high contact stresses, detailed studies must be made of application, loading, and manufacturing procedures to determine the desirable gradients of hardness, strength, and internal residual stresses throughout the tooth.

A guide for minimum case depth for nitrided teeth, based on the depth of maximum shear from contact loading, is given by

$$h_c = \frac{C_G U_c s_c d \sin \phi_o}{(1.66 \times 10^7)(\cos \psi_b)} \tag{35.80}$$

where h_c = minimum total case depth in inches and U_c = core hardness coefficient, from Fig. 35.43.

If the value of h_c from Eq. (35.80) is less than the value from Fig. 35.44, then the minimum value from Fig. 35.44 should be used. The equation for the lower or left-hand curve in Fig. 35.44 is

$$h_c = (4.328\,96)(10^{-2}) - P_{nd}(9.681\,15)(10^{-3}) + P_{nd}^2(1.201\,85)(10^{-3}) - P_{nd}^3(6.797\,21)(10^{-5}) + P_{nd}^4(1.371)(10^{-6}) \tag{35.81}$$

The equation of the right-hand curve is

$$h_c = (6.600\,90)(10^{-2}) - P_{nd}(1.622\,24)(10^{-2}) + P_{nd}^2(2.093\,61)(10^{-3}) - P_{nd}^3(1.177\,55)(10^{-4}) + P_{nd}^4(2.331\,60)(10^{-6}) \tag{35.82}$$

Note that other treatments of the subject of allowable gear-tooth bending recommend that the value obtained from Table 35.6 or Fig. 35.41 be multiplied by 0.70 for teeth subjected to reversed bending. This is not necessary within the context of this analysis, since the rim thickness factor K_b accounts for reversed bending.

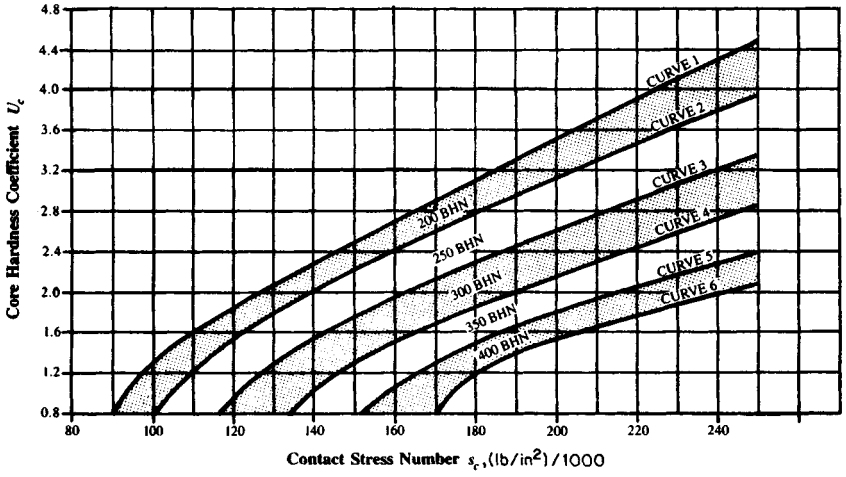

FIGURE 35.43 Core-hardness coefficient U_c as a function of the contact stress number s_c. The upper portion of the core-hardness bands yields heavier case depths and is for general design purposes; use the lower portion of the bands for high-quality material. *(From Ref. [35.1].)*

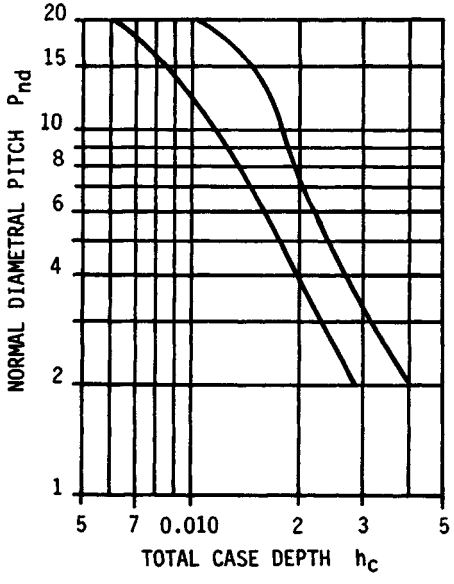

FIGURE 35.44 Minimum total case depth h_c for nitrided gears based on the normal diametral pitch. *(From Ref. [35.1].)*

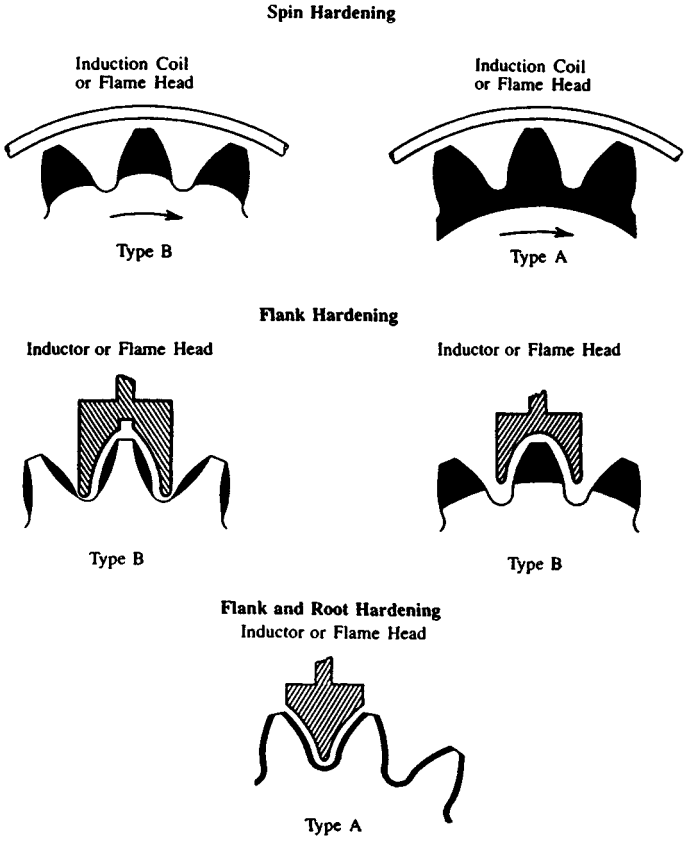

FIGURE 35.45 Variations in hardening patterns obtainable with flame or induction hardening. *(From Ref. [35.1].)*

For through-hardened gears, the yield stress at maximum peak stress should also be checked as defined by Eq. (35.83):

$$S_{ay}K_y \geq \frac{W_{t,\max}K_a}{K_v}\frac{P_d}{F}\frac{K_m}{K_f} \tag{35.83}$$

where $W_{t,\max}$ = peak tangential tooth load, lb
K_a = application factor
K_v = dynamic factor
F = minimum net face width, in
K_m = load-distribution factor
K_f = stress correction factor
K_y = yield strength factor
s_{ay} = allowable yield strength number, psi (from Fig. 35.46)

The yield strength factor should be set equal to 0.50 for conservative practice or to 0.75 for general industrial use.

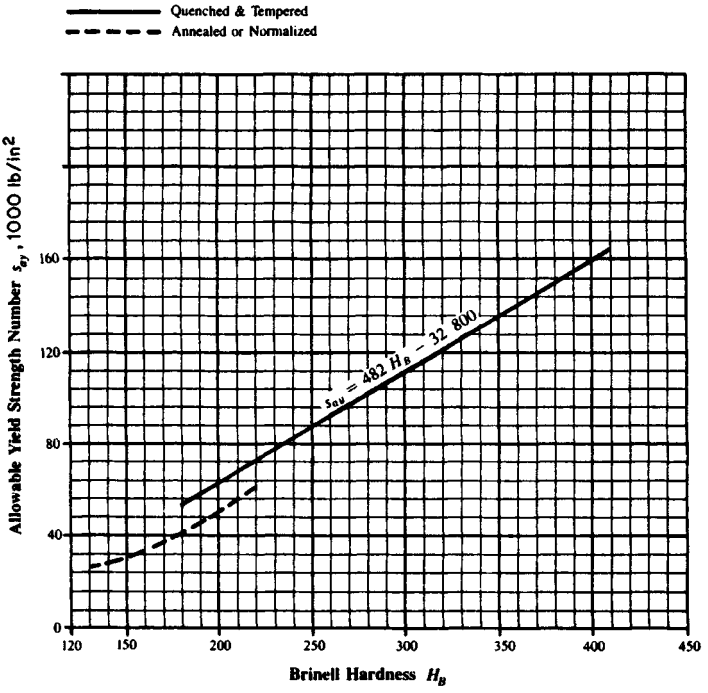

FIGURE 35.46 Allowable yield strength number s_{ay} for steel gears. *(From Ref. [35.1].)*

Hardness Ratio Factor $\mathbf{C_H}$. It is common practice in using through-hardened gear sets to utilize a higher hardness on the pinion than on the gear. The pinion typically sees many more cycles than the gear; thus a more economical overall design is obtained by balancing the surface durability and wear rate in this manner. Similarly, surface-hardened pinions may be used with through-hardened gears to provide improved overall capacity through the work-hardening effect which a "hard" pinion has on a "soft" gear. The hardness ratio factor adjusts the allowable stresses for this effect.

For through-hardened gear sets, C_H can be found from Fig. 35.47, while Fig. 35.48 provides values for surface-hardened pinions mating with through-hardened gears.

Life Factors $\mathbf{K_L}$ ***and*** $\mathbf{C_L}$. The allowable stresses shown in Tables 35.5 and 35.6 and Figs. 35.40 and 35.41 are based on 10 000 000 load cycles. The life factor adjusts the allowable stresses for design lives other than 10 000 000 cycles. A unity value for the life factor may be used for design lives beyond 10 000 000 cycles only when it is justified by experience with similar designs.

Insufficient specific data are available to define life factors for most materials. For steel gears, however, experience has shown that the curves shown in Figs. 35.49 and 35.50 are valid.

In utilizing these charts, care should be exercised whenever the product of K_L and s_{at} equals or exceeds s_{ay} as shown on Fig. 35.46, since this indicates that localized yielding may occur. For low-speed gears without critical noise vibration or transmis-

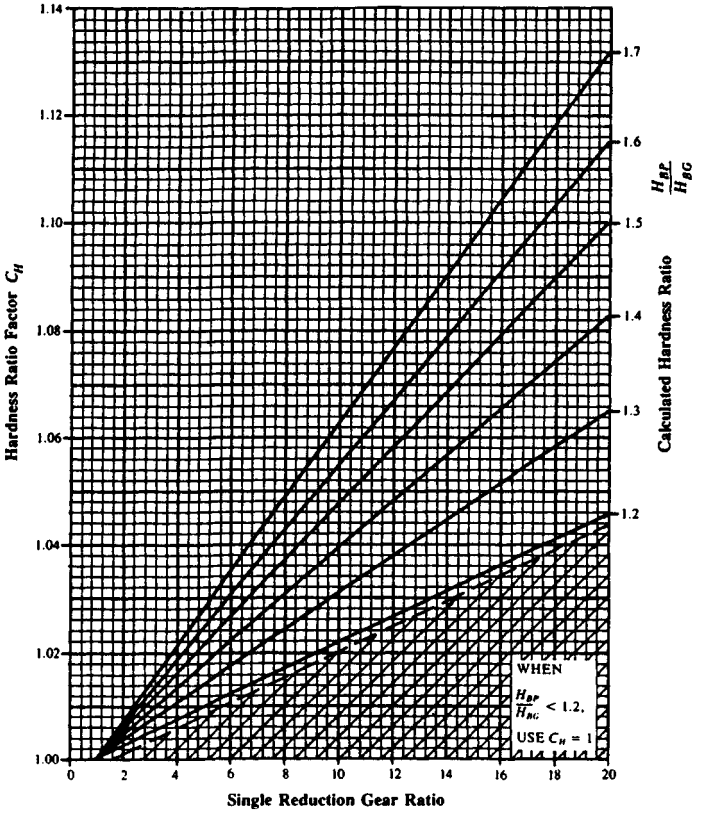

FIGURE 35.47 Hardness ratio factor C_H for through-hardened gears. In this chart, H_{BP} is the Brinell hardness of the pinion, and H_{BG} is the Brinell hardness of the gear. *(From Ref. [35.1].)*

sion accuracy requirements, local yielding may be acceptable, but it should be avoided in general.

***Reliability Factors* C_R *and* K_R.** The allowable stress levels are not absolute parameters. Rather, a specific probability of failure is associated with each allowable level. The values shown in Figs. 35.40 and 35.41 and Table 35.5 are based on a 99 percent probability of success (or a 1 percent probability of failure). This means that in a *large* population, at least 99 percent of the gears designed to a particular listed allowable stress will run for at least 10 000 000 cycles without experiencing a failure in the mode (that is, bending or durability) addressed.

In some cases it is desirable to design to higher or lower failure probabilities. Table 35.6 provides values for C_R and K_R which will permit the designer to do so. Before deciding on the reliability factor which is appropriate for a particular design, the analyst should consider what is meant by a "failure." In the case of a durability failure, a failure is said to have occurred when the first pit, or spall, is observed. Obviously a long time will elapse between the occurrence of a durability failure and the time at which the gear will cease to perform its normal power-transmission function.

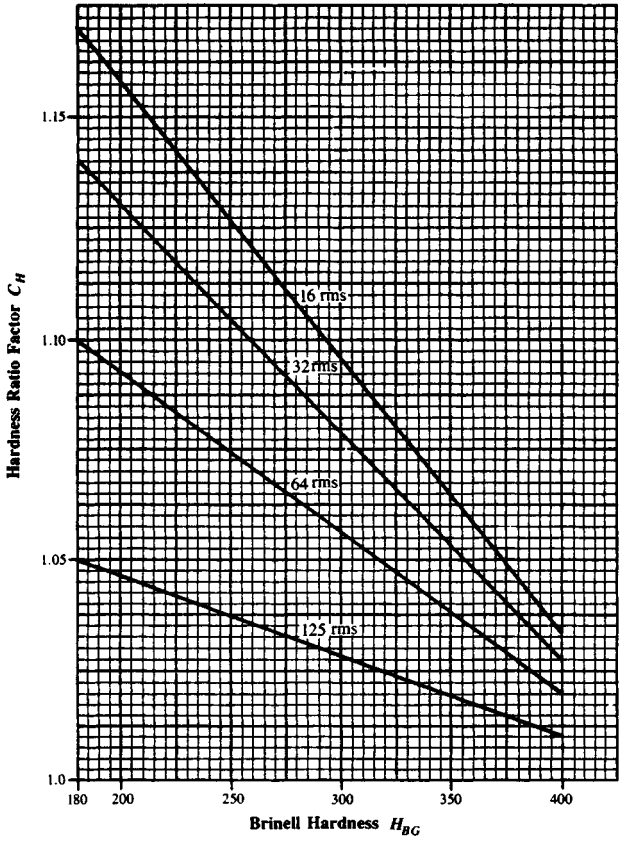

FIGURE 35.48 Hardness ratio factor C_H for surface-hardened teeth. The rms values shown correspond to the surface finish of the pinion f_p in microinches. *(From Ref. [35.1].)*

In the case of a bending failure, the appearance of a crack in the fillet area is the criterion. In most cases, and for most materials, the progression of this crack to the point at which a tooth or a piece of tooth fractures is rather quick. A bending failure will almost always progress to the point where function is lost much more rapidly than a durability failure. For this reason it is sometimes desirable to use a higher value for K_R than for C_R.

Because of the load sharing which occurs on most normal helical gears, a complete fracture of a full single tooth, as often occurs on a spur gear, is not usually the mode of failure on a helical gear. A certain redundancy is built into a helical gear, since initially only a piece of a tooth will normally fracture.

Temperature Factors $\mathbf{C_T}$ ***and*** $\mathbf{K_T}$**.** At gear blank operating temperatures below 250°F and above freezing, actual operating temperature has little effect on the allowable stress level for steel gears; thus a temperature factor of unity is used. At higher or lower temperatures, the allowable stress levels are altered considerably. Unfortunately, few hard data are available to define these effects. At very low tem-

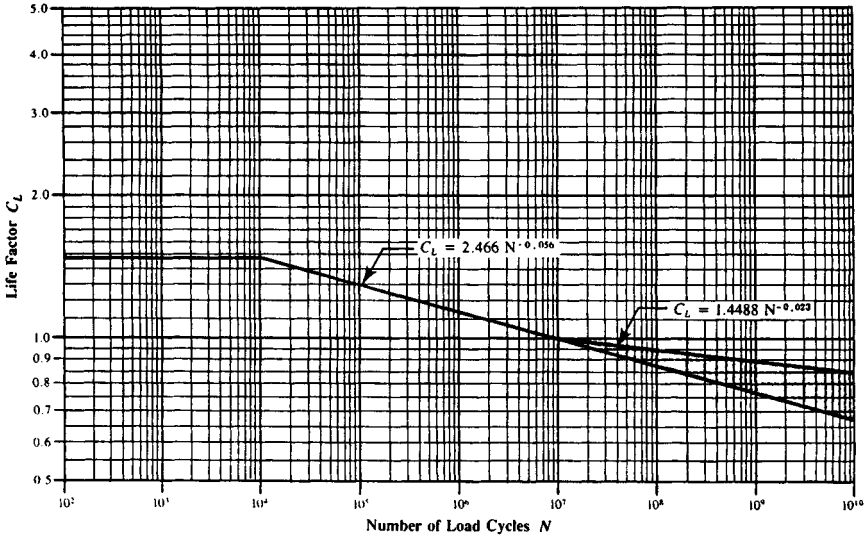

FIGURE 35.49 Pitting-resistance life factor C_L. This curve does not apply where a service factor C_{SF} is used. *Note:* The choice of C_L above 10^7 cycles is influenced by lubrication regime, failure criteria, smoothness of operation required, pitch line velocity, gear material cleanliness, material ductility and fracture toughness, and residual stress. *(From Ref. [35.1].)*

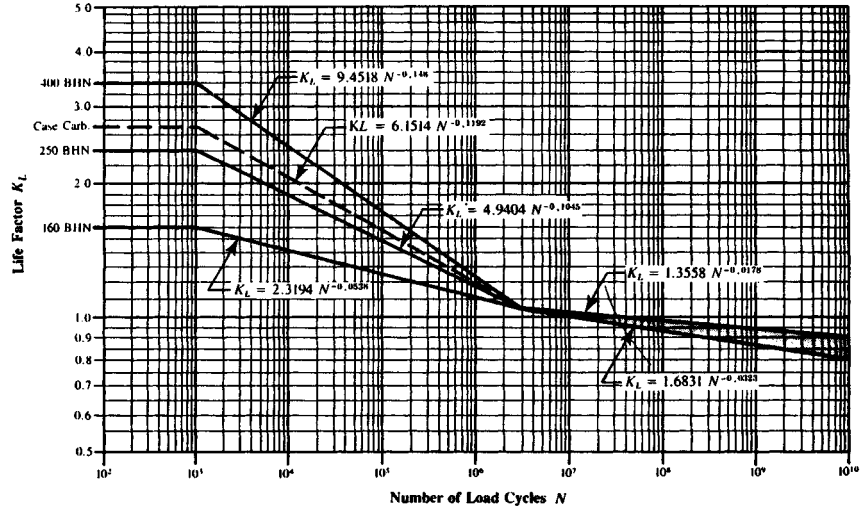

FIGURE 35.50 Bending-strength life factor K_L. This chart does not apply where a service factor K_{SF} is used. *Note:* The choice of K_L above 3×10^6 cycles is influenced by pitch line velocity, gear material cleanliness, residual stress, gear material ductility, and fracture toughness. *(From Ref. [35.1].)*

peratures, the impact resistance and fracture toughness of most materials are reduced; thus special care must be exercised in such designs if nonuniform loading is expected. A temperature factor greater than unity should be used in such cases. Although no specific data are available, a value between 1.25 and 1.50 is recommended for gears which must transmit full power between 0 and –50°F.

At high temperatures, most materials experience a reduction in hardness level. Nonmetallic gears are not ordinarily used at high temperatures; thus our comments are restricted to steel gearing. The temperature factor should be chosen on the basis of the hot hardness curve for the particular material in use. That is, the temperature factor is equal to the allowable stress at room-temperature hardness divided by the allowable stress at the hardness corresponding to the higher temperature. For information related to typical trends, Fig. 35.51 shows the hardness-temperature characteristics for two gear steels (AISI 9310 and VASCO-X2). Two typical bearing steels (M-50 and SAE 52100) are also shown for reference purposes.

Once the strength and durability analyses have been completed, the wear and scoring resistance of the gears must be defined. Wear (see Chap. 6) is usually a concern only for relatively low-speed gears, whereas scoring is a concern only for relatively high-speed gears.

Wear. Gear-tooth wear is a very difficult phenomenon to predict analytically. Fortunately, it is not a major problem for most gear drives operating in the moderate- to

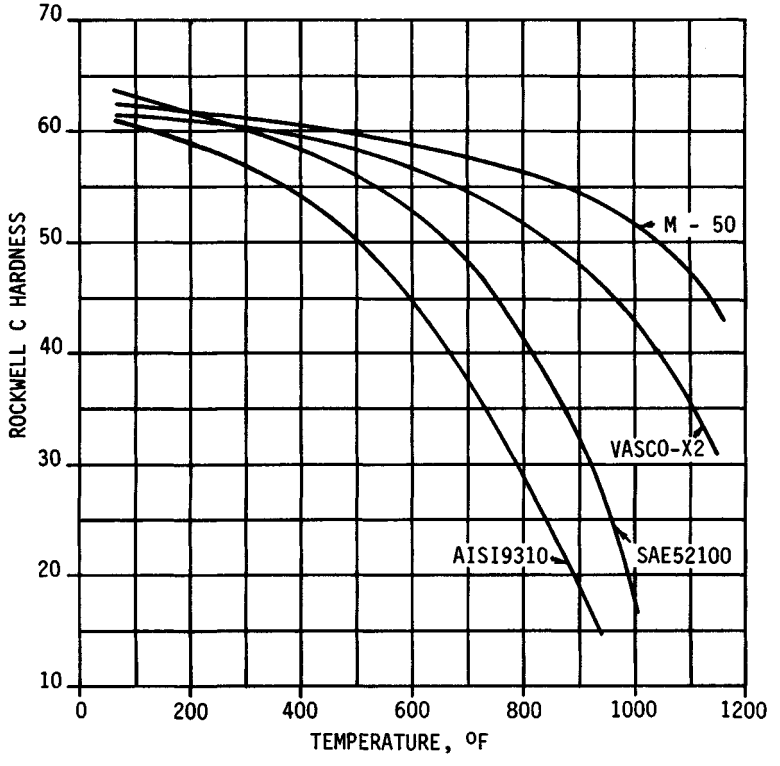

FIGURE 35.51 Hardness as a function of temperature for several steels.

high-speed range. In the case of low-speed gears, however, not only is wear a significant problem, but also it can be the limiting factor in defining the load capacity of the mesh.

In low-speed gear drives, the film which separates the mating tooth surfaces is insufficient to prevent metal-to-metal contact; thus wear occurs. In higher-speed gears, the film becomes somewhat thicker, and gross contact of the mating surfaces is prevented. Indeed, grinding lines are still visible on many aircraft gears after hundreds of hours of operation. The type of surface distress which will occur in a gear set is dependent, to a certain extent, on the pitchline velocity. As shown in Fig. 35.52, wear predominates in the lower-speed range, while scoring rules the upper-speed range. In the midrange, pitting controls the gear life.

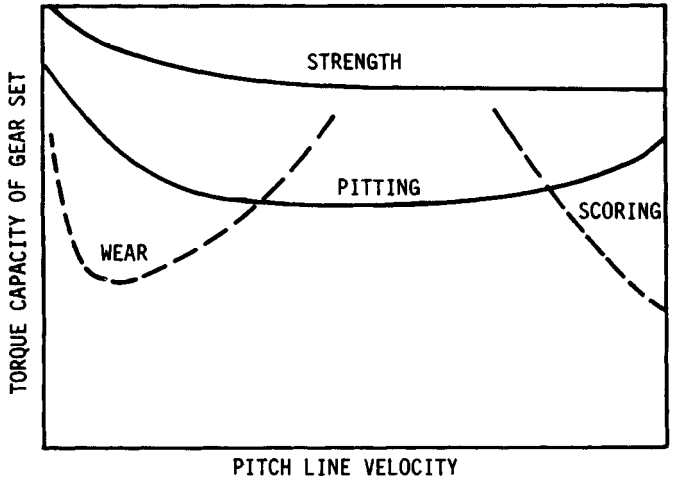

FIGURE 35.52 Gear distress as a function of pitch line velocity.

The elastohydrodynamic (EHD) film thickness can provide some guidance in the evaluation of the wear potential of a gear set. Care must be used in the application of these methods, since the existing data are far from complete and there are many instances of contradictory results. One of the simplest approaches is due to Dowson; see Ref. [35.7] and Chap. 25. The equation is

$$\frac{h}{R'} = \frac{(4.46 \times 10^{-5})(\alpha E')^{0.54}[\mu_o u/(E'R')]^{0.70}}{[w/(E'R')]^{0.13}} \tag{35.84}$$

where h = calculated minimum film thickness, in
R' = relative radius of curvature in transverse plane at pitch point, in
α = lubricant pressure-viscosity coefficient, in^2/lb
E' = effective elastic modulus, psi
μ_o = sump lubricant viscosity, centipoise (cP)
u = rolling velocity in transverse plane, inches per second (in/s)
w = load per unit length of contact, lb/in

Wellauer and Holloway ([35.8]) present a nomograph to compute the film thickness at the pitch point; but this nomograph is quite detailed and is not included here.

The parameter of interest in our discussion is not the film thickness itself, but rather the ratio of the film thickness to the relative surface roughness. This ratio is defined as the *specific film thickness* and is given by

$$\lambda = \frac{h}{S'} \tag{35.85}$$

The relative surface roughness [root-mean-square (rms)] is given by

$$S' = \frac{S_P + S_G}{2} \tag{35.86}$$

Typical values for various gear manufacturing processes are shown in Table 35.7.

TABLE 35.7 Tooth Surface Texture in the As-Finished Condition

Finish method	Surface texture in microinches (rms)	
	Range	Typical
Hobbed	30–80	50
Shaved	10–45	35
Lapped	20–200	93
Lapped and run in	20–100	53
Ground (soft)	5–35	25
Ground (hard)	5–35	15
Honed and polished	4–15	5

Once the specific film thickness has been determined, the probability of surface distress occurring can be determined through the use of Fig. 35.53.

Although the data presented thus far can be quite useful, several factors must be kept in mind in applying them to actual design. Most of the experimental data on which this information is based were obtained from through-hardened gear sets operating with petroleum-based oils. Gears operating with synthetic oils appear able to operate successfully at film thicknesses much less than those predicted by this analysis. The same is true for case-hardened gears of 59 R_C and higher hardness. The results may be further altered by the use of friction modifiers or EP additives in the oil. Finally, wear, of and by itself, is not necessarily a failure. In many cases, wear is an acceptable condition; it is simply monitored until it reaches some predetermined level, at which time the gears are replaced.

Perhaps the most useful application for this analysis is as a comparative, relative rating tool, rather than as an absolute design criterion.

The occurrence of wear is difficult to predict, but the rate of wear is even more so. Equation (35.87) may be useful as a guide in predicting wear, but its accuracy has not been rigorously verified:

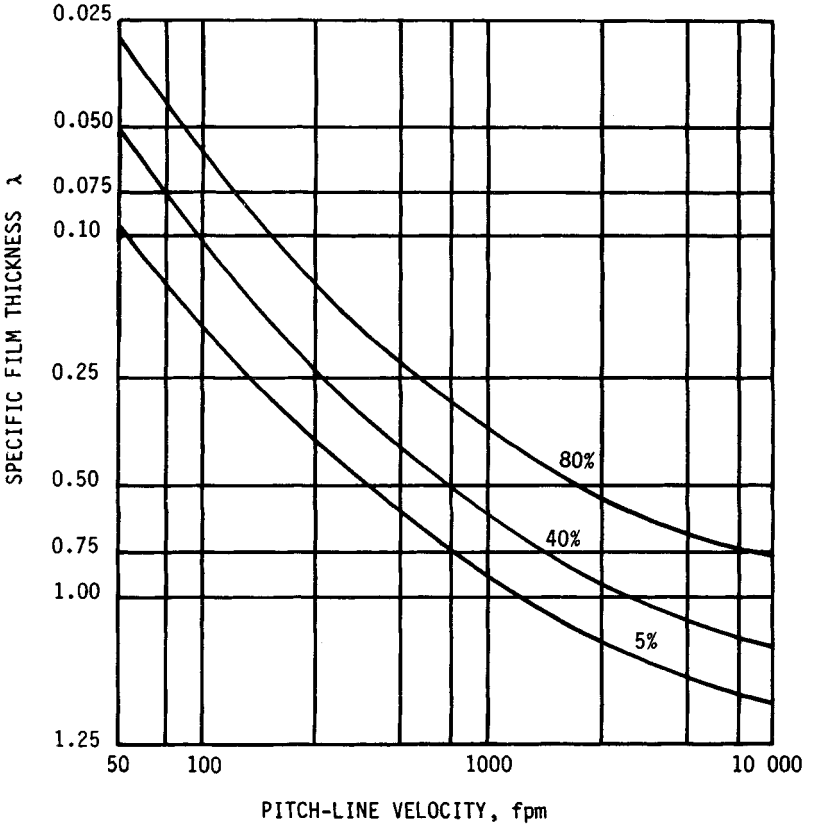

FIGURE 35.53 Surface-distress probability chart as a function of pitch line velocity and specific film thickness. Curves represent 80, 40, and 5 percent probability of distress. The region above the 80 percent line is unsatisfactory; the region below the 5 percent line is good.

$$q = \frac{KW_t n_T}{FS_y} \tag{35.87}$$

where q = wear, in
n_T = number of cycles
S_y = yield strength of gear material, psi
K = factor from Eq. (35.88)

and

$$3.1 \geq K\lambda^{1.645} \times 10^9 \geq 1.8 \tag{35.88}$$

In applying these equations, greater emphasis should be placed on the trend indicated than on the absolute value of the numbers. For example, a new design might be compared with an existing similar design for which the wear characteristics have been established. This could be accomplished by calculating the q value for each by

Eqs. (35.87) and (35.88) and then comparing them, rather than looking at absolute values of either. The ratio of the two q values is far more accurate than the absolute value of either.

Scoring. Very few data concerning the scoring behavior of gears are available in an easily usable form. Scoring is normally a problem for heavily loaded, high-speed steel gears. The exact mechanism by which scoring occurs is not yet fully understood.

At high speeds, the calculated film thickness is often quite large. Yet a wearlike failure mode sometimes occurs. Under high-speed conditions, the sliding motion of one gear tooth on another may create instantaneous conditions of temperature and pressure which destroy the film of oil separating the tooth flanks. When this occurs, the asperities on the surfaces of the mating teeth instantaneously weld. As the gears continue to rotate, these welds break and drag along the tooth flanks, causing scratches, or "score" marks, in the direction of sliding. If the damage which occurs is very slight, it is often referred to as *scuffing* or *frosting.* In some cases, light frosting may heal over and not progress; however, scoring is generally progressively destructive. Though never a catastrophic failure itself, scoring destroys the tooth surface, which leads to accelerated wear, pitting, and spalling. If scoring is allowed to progress unchecked, tooth fracture may ultimately occur.

Note that scoring is not a fatigue phenomenon; that is, its occurrence is not time-dependent. In general, if scoring does not occur within 15 to 25 minutes (min) at a certain operating condition, usually it will not occur *at that condition* at all. Only a change in operating condition, and not the accumulation of cycles, will cause scoring.

A theory known as the *critical-temperature theory,* originally proposed by Harmen Blok, is usually used in the evaluation of scoring hazard for a set of helical gears.

If we consider a simple analogy, the concept of critical temperature will become clear. Consider the old method of making fire by rubbing two sticks together. If the sticks are held together with only light pressure and/or they are rubbed slowly, they will simply wear. If, however, the pressure is increased and the sticks are rubbed more rapidly, then the temperature at the mating surfaces will increase. If the pressure (load) and the rubbing speed (sliding velocity) are progressively increased, eventually the sticks will ignite. At the point of ignition, the sticks have reached their *critical* temperature. Quite obviously, the critical temperature will vary with the type of wood, its moisture content, and other factors.

In a similar manner, as gear-tooth sliding velocity and load are increased, eventually a point will be reached at which the temperature at the conjunction attains a critical value, and then the film separating the tooth flanks will be destroyed. At this point the teeth are in metal-to-metal contact, and instantaneous welding of the surface asperities occurs. The continued rotation of the mesh rips apart these microscopic welds and produces the scored appearance from which this failure derives its name. The critical temperature varies with the type of gear material, surface hardness, surface finish, type and viscosity of oil, additives in the oil, etc. When the film is destroyed, it is sometimes referred to as *flashing;* thus the parameter used to evaluate this condition has come to be known as the *flash* temperature. When the flash temperature reaches its *critical* value, failure by scoring will occur. Note that the flash temperature referred to here is not related in any way to the flash point of the oil; and the oil flash point shown on some manufacturers' specification sheets is in no way related to the allowable flash temperature discussed here.

Many refinements have been made to Blok's original theory, and it is currently accepted as the best method available for evaluating scoring resistance for spur, helical, and bevel gears. Reference [35.9] presents a method of analysis for steel spur and

helical gears based on Blok's method. The scoring hazard is evaluated by calculating a flash temperature rise ΔT_{Fi}. The flash temperature rise is added to the gear blank temperature T_B and compared with the allowable tooth flash temperature for the particular material and lubricant combination being used.

The flash temperature rise is given by

$$\Delta T_{Fi} = \left(\frac{W_{ti} C_a C_m}{F C_v}\right)^{0.75} \left(\frac{n_P^{0.5}}{P_d^{0.25}}\right) (\mu Z_{ti}) \left(\frac{50}{50 - S'}\right) \tag{35.89}$$

where T_{Fi} = flash temperature rise at ith contact point along line of action, °F
W_{ti} = tangential tooth load at ith contact point, lb
F = net minimum face width, in
C_a = application factor
C_m = load-distribution factor
C_v = dynamic factor
n_P = pinion speed, revolutions per minute (r/min)
P_d = transverse diametral pitch
S' = relative surface roughness, Eq. (35.86)
Z_{ti} = scoring geometry factor at ith contact point along line of action

The factors C_a, C_v, and C_m are the same as those used in the durability formula [Eq. (35.17)].

The scoring geometry factor is given by

$$Z_{ti} = \frac{0.2917[\rho_{Pi}^{1/2} - (N_P \rho_{Gi}/N_G)^{1/2}] P_d^{1/4}}{(\cos \phi_i)^{0.75} [\rho_{Pi} \rho_{Gi}/(\rho_{Pi} + \rho_{Gi})]^{0.25}} \tag{35.90}$$

where ρ_{Pi}, ρ_{Gi} = radius of curvature of pinion and gear, respectively, at ith contact point, in
N_P, N_G = tooth numbers of pinion and gear, respectively
P_d = transverse diametral pitch
ϕ_i = pressure angle at ith contact point, deg

The tooth flash temperature is then calculated by

$$T_{Fi} = T_B + \Delta T_{Fi} \tag{35.91}$$

TABLE 35.8 Allowable Flash Temperatures for Some Gear Materials and for Spur and Helical Gears

The surface hardness is 60 R_C for all materials listed.

Gear material	Oil type	Allowable flash temperature, °F
AISI 9310	MIL-L-7808	295
	MIL-L-23699	295
	XAS 2354	335†
VASCO-X2	MIL-L-7808	350
	MIL-L-23699	350
	XAS 2354	375†

†Conservative estimate based on limited current data.

In most cases the blank temperature will be very close to the oil inlet temperature. Thus, unless the actual blank temperature is known, the oil inlet temperature may be used for T_B. Table 35.8 gives allowable values of the total flash temperature.

Equations (35.89) through (35.91) refer to the *i*th contact point. In utilizing these equations, the entire line of contact should be examined on a point-by-point basis to define the most critical contact point. Depending on the pitch of the tooth, 10 to 25 divisions should be adequate. For hand calculations, this could be quite burdensome. A quick look at the highest and lowest points of single-tooth contact (based on a transverse-plane slice of the helical set) will provide a reasonable approximation.

The range of materials and oils shown in Table 35.8 is limited. Generally, scoring is a problem only in high-speed, high-load applications.

The most likely applications to be affected are aerospace types. This being the case, the material choice is limited to those shown, and usually either MIL-L-23699 or MIL-L-7808 oil is used. Some of the new XAS-2354 oils will provide much improved scoring resistance, but hard data are not presently available.

REFERENCES

35.1 ANSI/AGMA 2001-B88, 1988, "Fundamental Rating Factors and Calculation Methods for Involute Spur and Helical Gear Teeth."

35.2 "Design Guide for Vehicle Spur and Helical Gears," AGMA publ. 170.

35.3 *Gear Handbook,* vol. 1, *Gear Classification, Materials, and Measuring Methods for Unassembled Gears,* AGMA publ. 390.

35.4 Raymond J. Drago, "Results of an Experimental Program Utilized to Verify a New Gear Tooth Strength Analysis," AGMA publ. 229.27, October 1983.

35.5 Raymond J. Drago, "An Improvement in the Conventional Analysis of Gear Tooth Bending Fatigue Strength," AGMA publ. 229.24, October 1982.

35.6 R. Errichello, "An Efficient Algorithm for Obtaining the Gear Strength Geometry Factor on a Programmable Calculator," AGMA publ. 139.03, October 1981.

35.7 D. Dowson, "Elastohydrodynamic Lubrication: Interdisciplinary Approach to the Lubrica-tion of Concentrated Contacts," NASA SP-237, 1970.

35.8 E. J. Wellauer and G. Holloway, "Application of EHD Oil Film Theory to Industrial Gear Drives," ASME paper no. 75PTG-1, 1975.

35.9 "Information Sheet—Gear Scoring Design Guide for Aerospace Spur and Helical Involute Gear Teeth," AGMA publ. 217.